ACS Chemical Neuroscience

pubs.acs.org/chemneuro Research Article

From Methaqualone and Beyond: Structure−Activity Relationship of 6-, 7-, and 8-Substituted 2,3-Diphenyl-quinazolin-4(3*H*)-ones and in Silico Prediction of Putative Binding Modes of Quinazolin-4(3*H*)-ones as Positive Allosteric Modulators of $GABA_A$ Receptors

Peng-Fei Wang, Anders A. Jensen,* and Lennart Bunch*

Cite This: https://dx.doi.org/10.1021/acschemneuro.0c00600 Read Online

ACCESS | Metrics & More | Article Recommendations

ABSTRACT: Methaqualone (2-methyl-3-(*o*-tolyl)-quinazolin-4(3*H*)-one, MTQ) is a moderately potent positive allosteric modulator (PAM) of $GABA_A$ receptors ($GABA_ARs$). In a previous structure−activity relationship (SAR) study probing the importance of 2- and 3-substituents in the quinazolin-4(3*H*)-one scaffold, several potent $GABA_AR$ PAMs were identified, including 2,3-diphenylquinazolin-4(3*H*)-one (PPQ) and 3-(2-chlorophenyl)-2-phenylquinazolin-4(3*H*)-one (Cl-PPQ). Here, PPQ was applied as lead in a SAR study of 6-, 7-, and 8-substituents in the quinazolin-4(3*H*)-one by synthesis and functional characterization of 36 PPQ analogs at various $GABA_AR$ subtypes. While none of the new analogs were significantly more potent than PPQ or displayed pronounced subtype selectivity across the $GABA_ARs$ tested, several interesting SAR observations were extracted from the study. In an *in silico* study, the putative binding modes of MTQ, PPQ, and Cl-PPQ in the transmembrane $\beta_2^{(+)}/\alpha_1^{(-)}$ interface of the $\alpha_1\beta_2\gamma_{2S}$ $GABA_AR$ were predicted. Several plausible binding modes were identified for the three PAMs, and rationalization of the molecular basis for their different modulatory potencies was attempted.

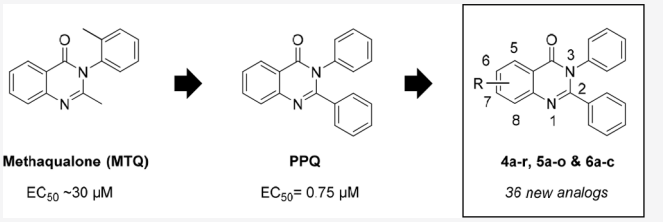

KEYWORDS: *$GABA_A$ receptors, $GABA_A$ positive allosteric modulators (PAMs), structure−activity relationship (SAR) study, methaqualone, transmembrane domain, docking*

INTRODUCTION

γ-Aminobutyric acid (GABA) is the major inhibitory neurotransmitter in the CNS, where it mediates its fast signaling through the $GABA_A$ receptors ($GABA_ARs$).[1,2] The $GABA_AR$ is a membrane-embedded complex assembled from five subunits, and it is composed of an extracellular domain (ECD) made up by the *N*-termini of the five subunits, a transmembrane domain (TMD) consisting of the four transmembrane α-helices (TM1−4) from each of the subunits, and an intracellular domain made up by the intracellular loops in the subunits.[3,4] A total of 19 subunits ($\alpha_1-\alpha_6$, $\beta_1-\beta_3$, $\gamma_1-\gamma_3$, δ, ε, π, θ, $\rho_1-\rho_3$) form the basis for the highly heterogeneous family of different pentameric $GABA_AR$ complexes, which are typically assembled from two α subunits, two β subunits and one additional subunit, with $\alpha\beta\gamma_2$ assemblies being by far the most predominant $GABA_ARs$, organized in a counterclockwise $^{(-)}\beta^{(+)}/^{(-)}\alpha^{(+)}/^{(-)}\beta^{(+)}/^{(-)}\alpha^{(+)}/^{(-)}\gamma^{(+)}$ arrangement (from the extracellular perspective).[1,2,5,6] At least 30 different $GABA_AR$ subtypes are expressed throughout the brain, and the sheer abundance and the essential roles governed by them as regulators of neuronal excitability make them highly attractive drug targets in a wide range of psychiatric, cognitive, and neurodegenerative disorders. To date, this huge therapeutic potential has partly been realized through the development of drugs for sleep disorders, anxiety/depression, and epilepsy.[7−13] On the other hand, the adverse effects exhibited by the current $GABA_AR$ therapeutics have also been ascribed to these multiple native $GABA_AR$ subtypes and the fairly broad modulation of these exerted by the drugs. Thus, medicinal chemistry efforts in the $GABA_AR$ field are often focused on the identification and development of novel ligands characterized by distinct modulatory properties or more discrete subtype-selectivity profiles compared to the existing drugs.[7,9,14−16]

GABA mediates its signaling through the $GABA_AR$ via binding to two orthosteric sites in the extracellular $\beta^{(+)}/\alpha^{(-)}$ interfaces of the pentameric complex, which also contains multiple allosteric sites targeted by numerous modulators.[2,17,18] These sites are located in the ECD (e.g., targeted by benzodiazepines) as well as in the TMD (e.g., targeted by

Received: September 15, 2020
Accepted: October 21, 2020

general anesthetics and neurosteroids), with one of the most explored allosteric sites residing in the $\beta^{(+)}/\alpha^{(-)}$ interface of the $GABA_AR$ TMD.[2,17,18] This interface is targeted by a plethora of different modulators, including the general anesthetic etomidate and the anticonvulsant loreclezole,[19−31] of which many exhibit pronounced selectivity for β_2/β_3-containing over β_1-containing $GABA_AR$ subtypes. The binding cavity is formed by TM2 and TM3 from the β subunit and TM1 and TM2 from the α subunit, and a couple of residues have been shown to line the modulator binding site (β_2-Met^{286}, α_1-Met^{236}) or to function as a transducer element between modulator binding and effect on gating (β_2-Asn^{265}).[20,22−24,27,28,30−32]

In two previous studies, we have pursued the potential of quinazolin-4(3*H*)-one-based allosteric modulators of $GABA_ARs$. Our interest in this scaffold was kindled with the discovery that methaqualone (2-methyl-3-(*o*-tolyl)-quinazolin-4(3*H*)-one, MTQ), a hypnotic-sedative and infamous recreational drug from the 1960 and 1970s, is a positive allosteric modulator (PAM) of $GABA_ARs$.[33] Based on the structural similarity of MTQ to etomidate and loreclezole and delineation of the impact of mutations of the β_2-Asn^{265}, β_2-Met^{286}, and α_1-Met^{236} residues on its $GABA_AR$ modulation, we proposed that MTQ acts through the $\beta^{(+)}/\alpha^{(-)}$ TMD interface in the receptor.[33] In a subsequent elaborate structure−activity relationship (SAR) study of 67 commercially available MTQ analogs wherein the 2- and 3-substituents on the quinazolin-4(3*H*)-one ring were varied systematically, the introduction of a 2-aryl ring substituent was found to lead to a significant increase in modulatory potency. Thus, the analog 2,3-diphenylquinazolin-4(3*H*)-one (PPQ) displayed 40−120-fold increases in modulatory potency compared to MTQ across $\alpha_{1,2,3,4,5}\beta_2\gamma_{2S}$ $GABA_ARs$ in the fluorescence-based FLIPR Membrane Potential Blue (FMP) assay (Table 1), and the *ortho*-chloro PPQ analog 2-phenyl-3-(*o*-chlorophenyl)quinazolin-4(3*H*)-one (Cl-PPQ) exhibited 5−12-fold further increased modulatory potencies at these subtypes compared to PPQ in this assay (Table 1, Figure 1).[34]

Table 1. Functional Properties Exhibited by MTQ, PPQ, and Cl-PPQ at Human $\alpha_1\beta_2\gamma_{2S}$, $\alpha_3\beta_2\gamma_{2S}$, $\alpha_4\beta_2\gamma_{2S}$, and $\alpha_5\beta_2\gamma_{2S}$ $GABA_ARs$ Transiently Expressed in tsA201 Cells in the FMP Assay[a]

	EC_{50} (μM)			
compd	$\alpha_1\beta_2\gamma_{2S}$	$\alpha_3\beta_2\gamma_{2S}$	$\alpha_4\beta_2\gamma_{2S}$	$\alpha_5\beta_2\gamma_{2S}$
MTQ	∼30	∼30	∼30	∼30
PPQ	0.75	0.84	0.23	0.57
Cl-PPQ	0.079	0.069	0.045	0.063

[a]The modulators were co-applied with GABA EC_{10} (determined on the day of the experiment) for the respective receptor subtypes (i.e., no preincubation with the modulators). Data are from ref 34.

In the present study, we extend our SAR explorations of the quinazolin-4(3*H*)-one class of $GABA_AR$ PAMs using the 2,3-diaryl analog PPQ as a valuable new parental scaffold in a semirational and systematic SAR study of substituents in quinazolin-4(3*H*)-one positions 6, 7, and 8. Furthermore, based on an in silico study, we propose putative binding modes of MTQ, PPQ, and Cl-PPQ to the $\beta^{(+)}/\alpha^{(-)}$ interface of the $GABA_AR$ TMD and address the molecular basis for their different modulatory potencies.

RESULTS AND DISCUSSION

Even though the *ortho*-chloro PPQ analog Cl-PPQ in our previous study displayed somewhat higher potency as a $GABA_AR$ PAM than PPQ,[34] for synthetic simplicity, we decided to conduct the SAR study on positions 5−8 using PPQ as the parental scaffold.

Chemistry. Construction of the quinazolin-4(3*H*)-one core followed a previously reported procedure[35] whereby the appropriately substituted 2-amino benzoic acid (**1**) was first *N*-acylated to give the amide (**2**). Thereafter, this intermediate was cyclized to form the heterocycle **3**, which undergoes a condensation reaction with the appropriate aniline to form 2,3-substituted quinazolin-4(3*H*)-ones (**4**) (Scheme 1). Generally, the procedure worked smoothly for substituents in positions 6, 7, and 8, with overall yields ranging from moderate to high. However, we failed to synthesize 5-chloro-2,3-diphenylquinazolin-4(3*H*)-one, as cyclization of intermediate 2-benzamido-6-chloro-*N*-phenylbenzamide did not proceed accordingly. Other commonly used approaches to prepare 2,3-diphenylquinazolin-4(3*H*)-ones, for example, solvent-free one-pot reaction assisted by microwave or changing acetic acid to pyridine, made no difference to the result.[36,37] We believe that the stereoelectronic impact of the chlorine atom with the carbonyl group prevents the formation of the planar ring structure **3** under the conditions tried.

The two 6- and 8-hydroxy analogs **5a** and **5b**, respectively, were obtained by saponification of their corresponding ester precursors (**4l** and **4m**,Scheme 2).

From the pool of analogs in hand, we identified 8-bromo analog **4p** as an attractive starting point to explore the SAR of the 8 position in even more detail. Thus, by means of three palladium coupling procedures, 13 additional 8-substituted analogs (**5c−o**) were prepared (Scheme 3). On the synthesis of **5l**, an unexpected condensation reaction of the product with DMF took place in situ to give product **5m** (Scheme 4).[38] However, by shortening the reaction time from 18 to 8 h, we were able to isolate target compound **5l**.

To increase the diversity of compounds for pharmacological characterization even further, **5l** was hydrolyzed to give acid **6a**. With the unexpected analog **5m** in hand, we saw the opportunity to convert it to heterocycle **6b**, and finally **5k** was oxidized to ketone **6c** (Scheme 4).

A total of 36 substituted 2,3-diphenylquinazolin-4(3*H*)-one (PPQ) analogs were synthesized.

SAR. The functional properties of the 36 PPQ analogs synthesized were determined at human $\alpha_1\beta_2\gamma_{2S}$, $\alpha_3\beta_2\gamma_{2S}$, $\alpha_4\beta_2\gamma_{2S}$, and either $\alpha_5\beta_2\gamma_{2S}$ (15 of the 36 analogs) or $\alpha_6\beta_2\gamma_{2S}$ (21 of the 36 analogs) $GABA_ARs$ transiently expressed in tsA201 cells in the FMP assay (see Experimental Section for details). In the following, the functional properties of the analogs will be presented according to their respective substitution patterns on the quinazolin-4(3*H*)-one scaffold, with data divided into Tables 2, 3, 4, and 5 (6-substituted, 7-substituted, 8-substituted and disubstituted analogs, respectively).

For the 6-substituted analogs, a counterintuitive SAR profile was observed for **4a** (6-Cl), **4g** (6-Br), **4h** (6-OMe), and **4l** (6-NO_2), as addition of a halide or nitro group in this position was found to decrease the modulatory potency of PPQ by >30-fold at the receptors, whereas analog **4h** comprising the larger methoxy group only exhibited slightly reduced potency compared to PPQ across the subtypes (Table 2). Interestingly

https://dx.doi.org/10.1021/acschemneuro.0c00600
ACS Chem. Neurosci. XXXX, XXX, XXX−XXX

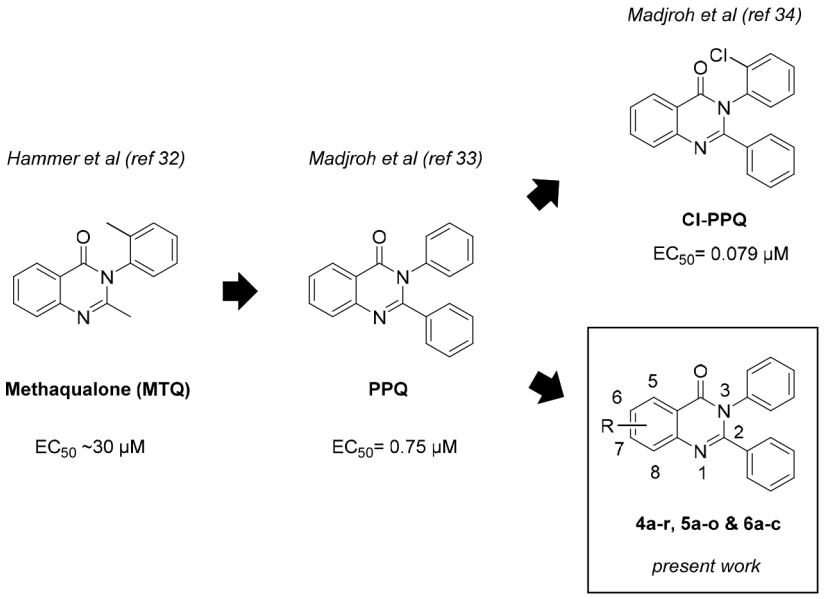

Figure 1. Chemical structures of MTQ, PPQ, Cl-PPQ, and 6,7,8-substituted PPQ analogs **4a−r**, **5a−o**, and **6a−c** presented in this study. The modulatory potencies exhibited by MTQ, PPQ, and Cl-PPQ at the $\alpha_1\beta_2\gamma_{2S}$ $GABA_AR$ transiently expressed in tsA-201 cells in the FMP assay are given.[34]

Scheme 1. Synthetic Route for Compounds 4a−r[a]

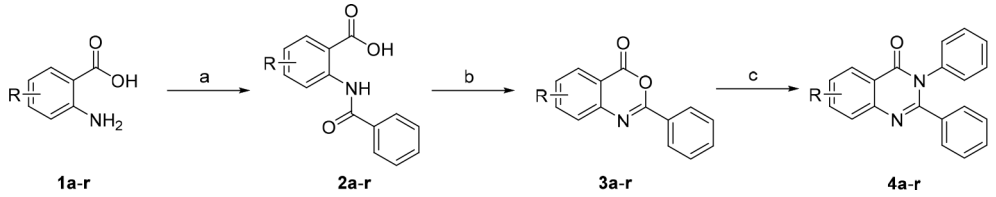

[a]Reagents and conditions: (a) BzCl, then TEA, DCM, 0 °C to rt, 5 h (90−96%); (b) Ac_2O, reflux, (84−92%); (c) aniline, AcOH, reflux, overnight (35−86%).

Scheme 2. Synthetic Routes for Compounds 5a−o[a]

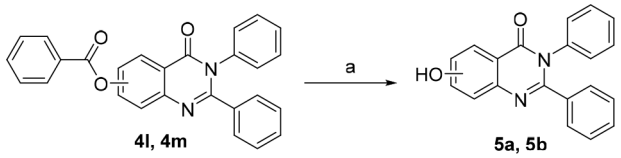

[a]Reagents and conditions: (a) KOH, H_2O, EtOH, 60 °C, 5 h (27−34%).

and in support of the activity of **4h**, **5a** (6-OH) also retained low micromolar potencies, which could point to the formation of a favorable hydrogen bond interaction between the OH/OMe group and the receptor, whereas larger substituents in the 6-position were not well-tolerated (**4j**, **4k**, and **4n**). The introduction of a chloro (**4b**) or a trifluoromethyl group (**4f**) in the 7-position of PPQ reduced $GABA_AR$ PAM activity substantially (Table 3).

The 8-substituted analogs offered the most interesting observations in this SAR study (Table 4). Analogously to the trend observed for the 6-substituted analogs, the 8-Cl analog (**4c**) and in particular the 8-Br analog (**4p**) were substantially weaker PAMs than PPQ, whereas the 8-OMe analog (**4r**) was equipotent with PPQ. While a general trend of 8-substituted analogs being slightly more potent PAMs at $\alpha_{4,5,6}\beta_2\gamma_{2S}$ over $\alpha_{1,3}\beta_2\gamma_{2S}$ receptors was observed, a 5−10-fold loss in modulatory potency was observed for the **4q** (8-F), **5b** (8-OH), and **5c** (8-Me) analogs at the latter receptor subtypes, and thus these analogs exhibited a preference (∼10-fold) for the $\alpha_{4,6}\beta_2\gamma_{2S}$ receptors. For the 8-alkyl analogs **5g−k**, a clear trend of smaller alkyl substituents being tolerated was observed, whereas increased bulkiness of the alkyl substituent decreased modulatory potencies across all receptor subtypes (**5g**,**i**,**j** and **6a**,**c** vs **5h**,**k**). A larger substituent was not well-tolerated (**4o**). The analogs **5d**, **5e**, **5f**, and **6b**, which all cotain heterocycles in the 8-position, presented interestingly diverse modulatory properties. While the presence of a lipophilic 3-thienyl group (**5b**) or a 2-methoxy pyrimidine group (**5f**) in this position lead to reduced PAM potency, the hydrogen bond accepting pyrimidine group in **5e** was better accommodated. Finally, introduction of a 5-amino-oxazole group in this position (**6b**) yielded another analog displaying ∼10-fold preference for $\alpha_{4,6}\beta_2\gamma_{2S}$ over $\alpha_{1,3}\beta_2\gamma_{2S}$ subtypes (Table 4). As for the three disubstituted analogs, **4d** and **4e**, which contain chloro in the 6- and 8-positions and in the 7- and 8-positions, respectively, exhibited significantly reduced PAM potency at all subtypes, whereas 6,7-dimethoxy analog **4i** was a weak PAM in the lower micromolar range with a preference for the $\alpha_{3,4,5}\beta_2\gamma_{2S}$ subtypes over $\alpha_{1,3}\beta_2\gamma_{2S}$ (Table 5).

In summary, none the 36 PPQ analogs exhibited significantly increased modulatory potencies compared PPQ, but analogs **4r**, **5a**, **5l**, **5o**, and **6c** retained the $GABA_AR$ PAM activity and were equipotent with the parent compound. While

https://dx.doi.org/10.1021/acschemneuro.0c00600
ACS Chem. Neurosci. XXXX, XXX, XXX−XXX

Scheme 3[a]

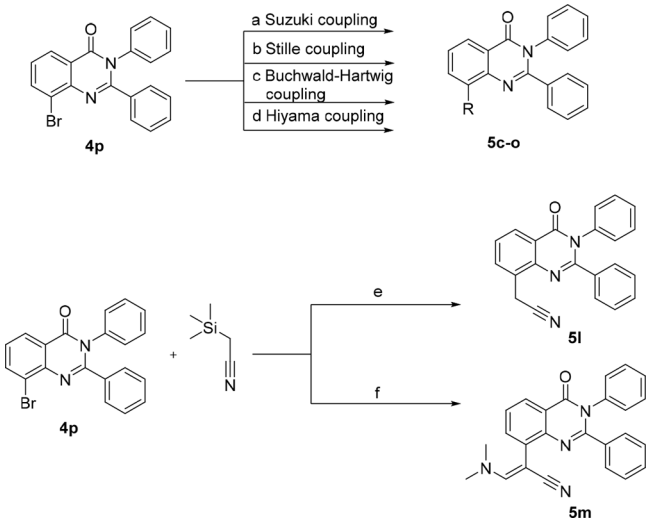

[a]Reagents and conditions: (a) $RB(OH)_2$, $Pd(PPh_3)_4$, Cs_2CO_3, toluene, Ar, 100 °C, overnight (43−78%); (b) RSn, $Pd(PPh_3)_4$, toluene, Ar, reflux, overnight, then KF, rt (31−55%); (c) morpholine, $Pd_2(dba)_3$, Xantphos, Cs_2CO_3, Ar, 100 °C, 4 h (43−77%); (d) 1,3,5-trimethoxybenzene, CsF, $Pd(PPh_3)_4$, 1,2-dichloroethane, acetyltrimethylsilane, Ar, 75 °C, 6 h (27%); (e) $Pd_2(dba)_3$, P(*t*-Bu)$_3$, ZnF_2, DMF, Ar, 90 °C, 8 h (47%); (f) $Pd_2(dba)_3$, P(*t*-Bu)$_3$, ZnF_2, DMF, Ar, 90 °C, 18 h (79%).

none of the analogs can be claimed to be subtype-selective PAMs, as mentioned above a couple of analogs that exhibited ∼10-fold preferences for some of the tested subtypes over others were identified.

Computational Study. An in silico study was performed to determine plausible binding modes of the quinazolin-4(3*H*)-one-based $GABA_AR$ PAMs and thereby strengthen the understanding of quinazolin-4(3*H*)-one SAR.[34] For this, the recently published cryo-EM structure of the engineered full-length $\alpha_1\beta_2\gamma_2$ $GABA_AR$ was employed (PDB code 6D6U).[39] Although this cryo-EM structure has a slightly lower resolution (3.9 Å) compared to available X-ray structures (5OJM and 5O8F at 3.3 and 3.2 Å, respectively), it comprises the α_1 and β_2 subunits, which are essential to the modeling study, and thus it is the best accessible template for this model. The built-in binding site identifier in MOE was applied, and the upper part of the cleft formed by the $\beta_2^{(+)}/\alpha_1^{(-)}$ interface in the $GABA_AR$ TMD was identified as the putative binding pocket. In detail, the binding pocket is located between $\beta_2^{(+)}$-TM2/TM3 and $\alpha_1^{(-)}$-TM1/TM2 α-helices (Figure 2A), and the residues lining the pocket are either neutral with hydrogen bonding capabilities or lipophilic (Figure 2B,C). This prediction fits well with the findings of our previous mutagenesis studies of the binding site of MTQ and its analogs,[33,34] as the binding pocket was lined by the β_2-TM3-Met^{286} and α_1-TM1-Met^{236} (Figure 3).

Binding Mode of MTQ in the $\beta_2^{(+)}/\alpha_1^{(-)}$ TMD Interface. Docking of MTQ into the $\beta_2^{(+)}/\alpha_1^{(-)}$ TMD interface resulted in five binding modes with comparable calculated scores *S* (predicted binding affinities) of −5.9 to −5.8 kcal/mol (Figure 3A,B), which differ in terms of how deep MTQ is inserted into the crevice between the β_2-TM3 and the α_1-TM2 helices but also with respect to the overall orientation of the molecule in the binding pocket (Figure 3A). The five binding modes can be divided into two general orientations. In two binding modes, the fused heterocycle of MTQ is oriented toward the ion channel (Figure 3A, green and purple). The binding mode depicted in green is clearly positioned deeper and closer to ion channel, whereas the binding mode shown in purple is facing the surrounding lipid bilayer. In the three other binding modes, the 3-(*o*-tolyl) and 2-methyl groups of MTQ are oriented toward the ion channel (Figure 3B, green, purple, and yellow). These three binding modes also differ with regard to how close MTQ is positioned relative to the ion channel. It is noted that the in silico predicted binding modes do not involve direct hydrogen bonding interactions between the carbonyl group and the aromatic nitrogen of MTQ and receptor residues. As specific water molecules are not identified in the cryo-EM structure, it remains unclear how these will affect binding mode or favor one binding mode over the others. Also an induced-fit mechanism may result in changes to the shape of the binding pocket.

Binding Mode of PPQ in the $\beta_2^{(+)}/\alpha_1^{(-)}$ TMD Interface. We next docked the more potent analog PPQ into the putative binding pocket. Analogously to the docking of MTQ, five binding modes for PPQ were identified, with scoring function *S* in the interval of −6.5 to −6.4 kcal/mol. The predicted binding modes of PPQ can be divided into three major orientations (Figure 4), none of which comprise specific hydrogen bonding interactions between PPQ and receptor

Scheme 4. Synthetic Routes for Compounds 6a−c[a]

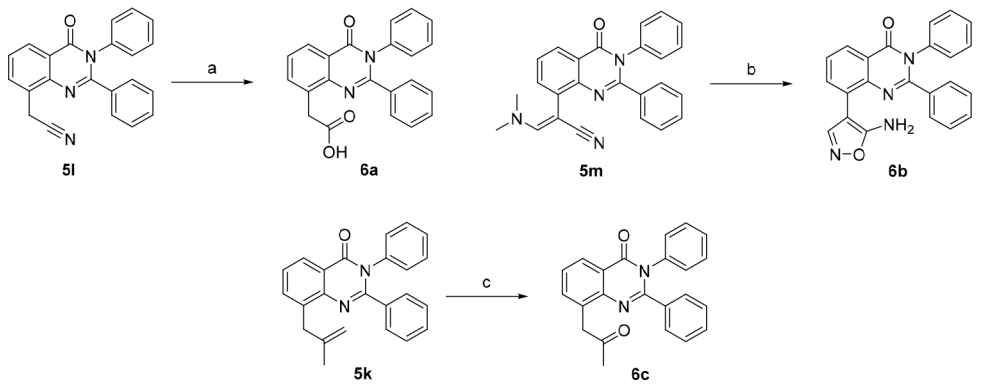

[a]Reagents and conditions: (a) KOH, H_2O, EtOH, 60 °C, 5 h (17%); (b) NH_2OH, EtOH, reflux, 1 h (82%); (c) OsO_4, THF/H_2O, 20 min, then $NaIO_4$, 16 h (63%).

https://dx.doi.org/10.1021/acschemneuro.0c00600
ACS Chem. Neurosci. XXXX, XXX, XXX−XXX

Table 2. Functional Properties Displayed by 6-Substituted PPQ Analogs at Human $\alpha_1\beta_2\gamma_{2S}$, $\alpha_3\beta_2\gamma_{2S}$, $\alpha_4\beta_2\gamma_{2S}$, $\alpha_5\beta_2\gamma_{2S}$, and $\alpha_6\beta_2\gamma_{2S}$ $GABA_A$Rs Transiently Expressed in tsA201 Cells in the FMP Assay[b]

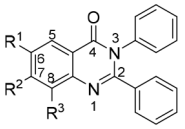

Cmpd	R^1	EC_{50} (μM) [pEC_{50} ± S.E.M.]				
		$\alpha_1\beta_2\gamma_{2S}$	$\alpha_3\beta_2\gamma_{2S}$	$\alpha_4\beta_2\gamma_{2S}$	$\alpha_5\beta_2\gamma_{2S}$	$\alpha_6\beta_2\gamma_{2S}$
PPQ	-H	0.75	0.84	0.23	0.57	nt
4a	-Cl	w.a.[a] *(6.25-100)*	w.a.[a] *(6.25-100)*	w.a.[a] *(25-100)*	w.a.[a] *(6.25-100)*	nt
4g	-Br	w.a.[a] *(25-100)*	w.a.[a] *(25-100)*	w.a.[a] *(6.25-100)*	w.a.[a] *(6.25-100)*	nt
4h	-OMe	5.5 [5.26 ± 0.10]	1.4 [5.84 ± 0.09]	1.4 [5.87 ± 0.11]	1.3 [5.89 ± 0.10]	nt
4j		w.a.[a] *(6.25-100)*	w.a.[a] *(6.25-100)*	w.a.[a] *(25-100)*	w.a.[a] *(6.25-100)*	nt
4k		w.a.[a] *(6.25-100)*	w.a.[a] *(25-100)*	w.a.[a] *(6.25-100)*	w.a.[a] *(6.25-100)*	nt
4l	$-NO_2$	w.a.[a] *(100)*	w.a.[a] *(25-100)*	w.a.[a] *(25-100)*	w.a.[a] *(100)*	nt
4n		w.a.[a] *(6.25-100)*	w.a.[a] *(25-100)*	w.a.[a] *(6.25-100)*	w.a.[a] *(25-100)*	nt
5a	-OH	1.3 [5.87 ± 0.17]	1.8 [5.75 ± 0.10]	1.62 [6.21 ± 0.08]	nt	0.45 [6.35 ± 0.09]

[a]w.a., weak activity. The concentration−response curve for the modulator was not completed within the concentration range tested. The modulator displayed significant effects at the concentration range indicated in the parentheses. [b]The modulators were co-applied with GABA EC_{10} (determined on the day of the experiment) for the respective receptor subtypes (i.e., no preincubation with the modulators). The data are based on 3−4 independent experiments (n = 3−4). nt, not tested.

Table 3. Functional Properties Displayed by 7-Substituted PPQ Analogs at Human $\alpha_1\beta_2\gamma_{2S}$, $\alpha_3\beta_2\gamma_{2S}$, $\alpha_4\beta_2\gamma_{2S}$, and $\alpha_5\beta_2\gamma_{2S}$ $GABA_A$Rs Transiently Expressed in tsA201 Cells in the FMP Assay[b]

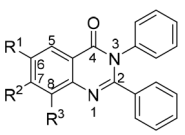

		EC_{50} (μM) [pEC_{50} ± SEM]				
compd	R^2	$\alpha_1\beta_2\gamma_{2S}$	$\alpha_3\beta_2\gamma_{2S}$	$\alpha_4\beta_2\gamma_{2S}$	$\alpha_5\beta_2\gamma_{2S}$	$\alpha_6\beta_2\gamma_{2S}$
4b	-Cl	w.a.[a] *(6.25−100)*	w.a.[a] *(6.25−100)*	w.a.[a] *(6.25−100)*	~10 [~5.0]	nt
4f	$-CF_3$	w.a.[a] *(25−100)*	w.a.[a] *(25−100)*	w.a.[a] *(25−100)*	w.a.[a] *(25−100)*	nt

[a]w.a., weak activity. The concentration−response curve for the modulator was not completed within the concentration range tested. The modulator displayed significant effects at the concentration range indicated in the parentheses. [b]The modulators were co-applied with GABA EC_{10} (determined on the day of the experiment) for the respective receptor subtypes (i.e., no preincubation with the modulators). The data are based on 3 independent experiments (n = 3). nt, not tested.

https://dx.doi.org/10.1021/acschemneuro.0c00600
ACS Chem. Neurosci. XXXX, XXX, XXX−XXX

Table 4. Functional Properties Displayed by 8-Substituted PPQ Analogs at Human $\alpha_1\beta_2\gamma_{2S}$, $\alpha_3\beta_2\gamma_{2S}$, $\alpha_4\beta_2\gamma_{2S}$, $\alpha_5\beta_2\gamma_{2S}$, and $\alpha_6\beta_2\gamma_{2S}$ $GABA_A$Rs Transiently Expressed in tsA201 Cells in the FMP Assay[b]

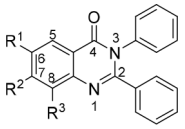

Cmpd	R^3	EC_{50} (μM) [pEC_{50} ± S.E.M.]				
		$\alpha_1\beta_2\gamma_{2S}$	$\alpha_3\beta_2\gamma_{2S}$	$\alpha_4\beta_2\gamma_{2S}$	$\alpha_5\beta_2\gamma_{2S}$	$\alpha_6\beta_2\gamma_{2S}$
PPQ	-H	0.75	0.84	0.23	0.57	nt
4c	-Cl	4.5 [5.34 ± 0.09]	5.3 [5.27 ± 0.08]	3.9 [5.41 ± 0.07]	3.8 [5.42 ± 0.08]	nt
4m	$-NO_2$	4.2 [5.38 ± 0.09]	w.a.[a] *(6.25-100)*	3.0 [5.52 ± 0.09]	4.6 [5.39 ± 0.04]	nt
4o		w.a.[a] *(25-100)*	w.a.[a] *(25-100)*	w.a.[a] *(25-100)*	w.a.[a] *(6.25-100)*	nt
4p	-Br	w.a.[a] *(10-100)*	w.a.[a] *(10-100)*	w.a.[a] *(30-100)*	nt	w.a.[a] *(30-100*
4q	-F	4.4 [5.35 ± 0.04]	2.1 [5.68 ± 0.08]	0.36 [6.44 ± 0.09]	nt	0.39 [6.41 ± 0.11]
4r	-OMe	0.44 [6.35 ± 0.11]	0.47 [6.32 ± 0.03]	0.13 [6.91 ± 0.06]	nt	0.12 [6.92 ± 0.06]
5b	-OH	3.8 [5.41 ± 0.11]	3.4 [5.46 ± 0.06]	0.44 [6.35 ± 0.05]	nt	0.27 [6.56 ± 0.11]
5c	-Me	3.4 [5.47 ± 0.04]	5.1 [5.30 ± 0.04]	0.66 [6.18 ± 0.08]	nt	0.54 [6.27 ± 0.11]
5d		w.a.[a] *(30-100)*	w.a.[a] *(30-100)*	w.a.[a] *(30-100)*	nt	w.a.[a] *(30-100)*
5e		2.2 [5.64 ± 0.11]	3.9 [5.40 ± 0.03]	2.1 [5.68 ± 0.08]	nt	0.58 [6.24 ± 0.10]
5f		w.a.[a] *(30-100)*	w.a.[a] *(30-100)*	w.a.[a] *(10-100)*	nt	w.a.[a] *(10-100)*
5g		6.5 [5.19 ± 0.08]	3.2 [5.49 ± 0.11]	3.3 [5.48 ± 0.09]	nt	1.8 [5.74 ± 0.12]
5h		w.a.[a] *(10-100)*	w.a.[a] *(3-100)*	w.a.[a] *(3-100)*	nt	w.a.[a] *(3-100)*
5i		2.5 [5.59 ± 0.06]	2.1 [5.68 ± 0.08]	0.78 [6.11 ± 0.09]	nt	0.58 [6.24 ± 0.10]
5j		3.5 [5.45 ± 0.06]	2.4 [5.61 ± 0.07]	1.3 [5.89 ± 0.06]	nt	1.4 [5.86 ± 0.11]
5k		w.a.[a] *(30-100)*	w.a.[a] *(10-100)*	w.a.[a] *(10-100)*	nt	w.a.[a] *(10-100)*

https://dx.doi.org/10.1021/acschemneuro.0c00600
ACS Chem. Neurosci. XXXX, XXX, XXX−XXX

Table 4. continued

5l		0.76 [6.12 ± 0.10]	0.64 [6.19 ± 0.03]	0.27 [6.56 ± 0.05]	nt	0.19 [6.71 ± 0.05]
5m		w.a.[a] *(100)*	w.a.[a] *(30-100)*	w.a.[a] *(30-100)*	nt	w.a.[a] *(30-100)*
5n		w.a.[a] *(30-100)*	w.a.[a] *(30-100)*	w.a.[a] *(10-100)*	nt	w.a.[a] *(10-100)*
5o		1.5 [5.81 ± 0.09]	1.1 [5.97 ± 0.13]	0.24 [6.63 ± 0.11]	nt	0.26 [6.58 ± 0.10]
6a		7.2 [5.14 ± 0.05]	7.6 [5.12 ± 0.07]	6.9 [5.16 ± 0.11]	nt	3.6 [5.44 ± 0.09]
6b		w.a.[a] *(3-100)*	5.6 [5.25 ± 0.13]	0.43 [6.37 ± 0.11]	nt	0.67 [6.17 ± 0.09]
6c		0.42 [6.37 ± 0.08]	0.71 [6.15 ± 0.11]	0.18 [6.75 ± 0.12]	nt	0.23 [6.64 ± 0.08]

[a]w.a., weak activity. The concentration−response curve for the modulator was not completed within the concentration range tested. The modulator displayed significant effects at the concentration range indicated in the parentheses. [b]The modulators were co-applied with GABA EC_{10} (determined on the day of experiment) for the respective receptor subtypes (i.e., no preincubation with the modulators). The data are based on 3−4 independent experiments (n = 3−4). nt, not tested.

Table 5. Functional Properties Displayed by Disubstituted PPQ Analogs at Human $\alpha_1\beta_2\gamma_{2S}$, $\alpha_3\beta_2\gamma_{2S}$, $\alpha_4\beta_2\gamma_{2S}$, and $\alpha_5\beta_2\gamma_{2S}$ $GABA_A$Rs Transiently Expressed in tsA201 Cells in the FMP Assay[b]

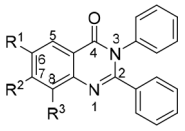

				EC_{50} (μM) [pEC_{50} ± SEM]				
compd	R^1	R^2	R^3	$\alpha_1\beta_2\gamma_{2S}$	$\alpha_3\beta_2\gamma_{2S}$	$\alpha_4\beta_2\gamma_{2S}$	$\alpha_5\beta_2\gamma_{2S}$	$\alpha_6\beta_2\gamma_{2S}$
4d	-Cl	-H	-Cl	w.a.[a] *(100)*	w.a.[a] *(25−100)*	w.a.[a] *(100)*	w.a.[a] *(100)*	nt
4e	-H	-Cl	-Cl	w.a.[a] *(25−100)*	w.a.[a] *(6.25−100)*	w.a.[a] *(25−100)*	w.a.[a] *(25−100)*	nt
4i	-OMe	-OMe	-H	w.a.[a] *(6.25−100)*	2.9 [5.53 ± 0.04]	6.1 [5.22 ± 0.07]	4.3 [5.37 ± 0.11]	nt

[a]w.a., weak activity. The concentration−response curve for the modulator was not completed within the concentration range tested. The modulator displayed significant effects at the concentration range indicated in the parentheses. [b]The modulators were co-applied with GABA EC_{10} (determined on the day of the experiment) for the respective receptor subtypes (i.e., no preincubation with the modulators). The data are based on 3−4 independent experiments (n = 3−4). nt, not tested.

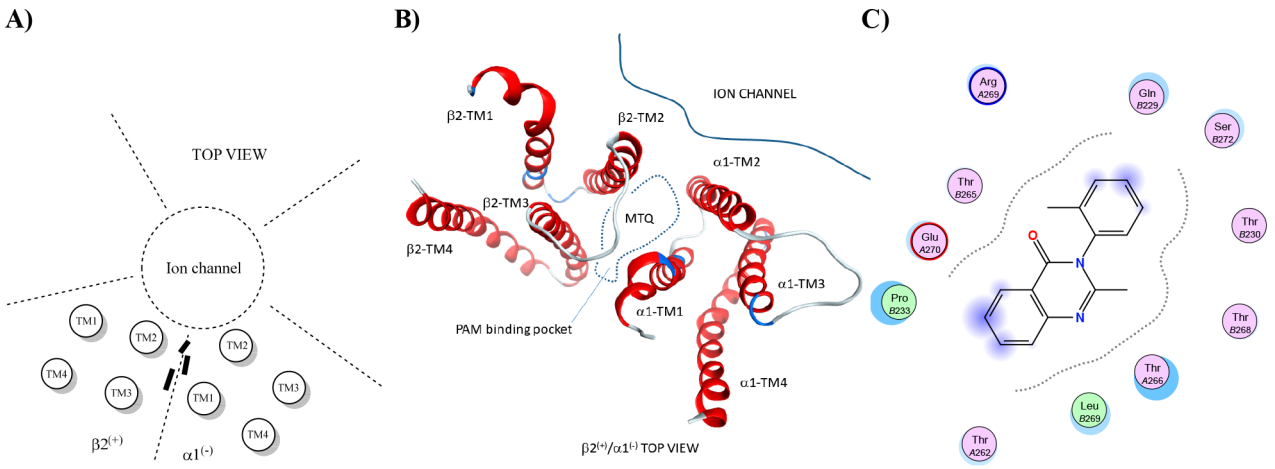

Figure 2. Putative binding pocket for the quinazolin-4(3*H*)-ones in the $\beta_2^{(+)}/\alpha_1^{(-)}$ interface of the $\alpha_1\beta_2\gamma_2$ $GABA_A$R TMD (PDB code 6D6U). (A) Top view schematic drawing of the $\alpha_1\beta_2\gamma_2$ $GABA_A$R TMD, with the four α-helices in a β_2 and an α_1 subunit indicated. The $\beta_2^{(+)}/\alpha_1^{(-)}$ TMD interface with the three identified binding modes of MTQ in the computational study is indicated. (B) 3-D structure of the $\beta_2^{(+)}/\alpha_1^{(-)}$ TMD interface. (C) Schematic drawing of the MTQ binding pocket in the $\beta_2^{(+)}/\alpha_1^{(-)}$ TMD interface with the residues lining the pocket indicated. PDB file, Chain A $\beta_2^{(+)}$; PDB file, Chain B $\alpha_1^{(-)}$. Green, apolar side chains; purple, polar side chains (red circle, acidic side chain; blue circle, basic side chain).

https://dx.doi.org/10.1021/acschemneuro.0c00600
ACS Chem. Neurosci. XXXX, XXX, XXX−XXX

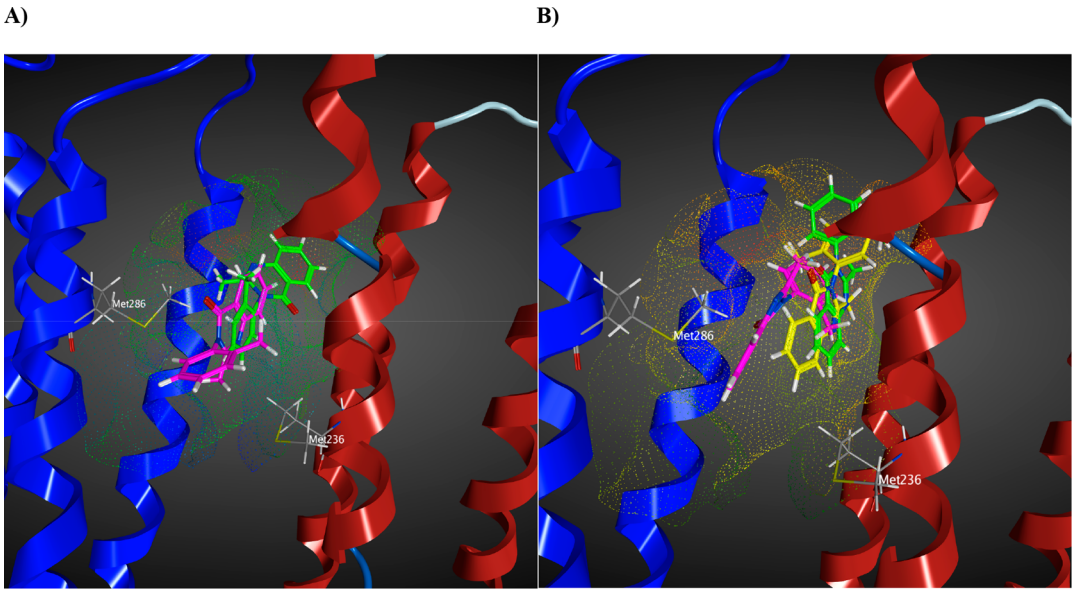

Figure 3. MTQ binding modes in the $\beta_2^{(+)}/\alpha_1^{(-)}$ TMD interface (blue and red helices, respectively). (A) Binding mode no. 1 of MTQ, projecting the fused heterocycle toward the ion channel. (B) Binding orientation no. 2 of MTQ, projecting the 3-(*o*-tolyl) and 2-methyl substituents toward the ion channel.

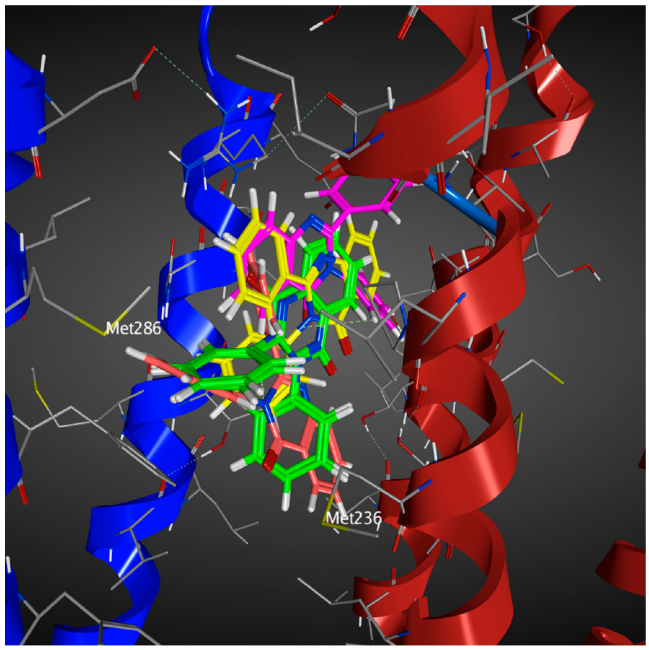

Figure 4. Superimposition of binding modes of PPQ in the $\beta_2^{(+)}/\alpha_1^{(-)}$ TMD interface. In PPQ, binding modes given in green (two modes, flipped) and yellow face the heterocyclic core faces toward the ion channel. The PPQ binding mode given in purple projects the two phenyl rings toward the ion channel. The PPQ binding mode given in orange is perpendicular in orientation. β_2 and α_1 helices are given in blue and in red, respectively.

residues. The 40−120-fold higher modulatory potencies of PPQ compared to MTQ, are not fully reflected in the calculated affinities of MTQ and PPQ, although the trend is confirmed (lower *S* value for PPQ). The substantially higher cLogP value of PPQ (4.75) compared to MTQ (3.65) can at least in part explain the higher potency of PPQ, but the process of mutually induced fit between ligand and host is complex and thus cannot be determined in detail from the present in silico study.

To validate the cogency of the in silico predicted binding modes for MTQ and PPQ in the wild-type $\beta_2^{(+)}/\alpha_1^{(-)}$ TMD interface, we next performed docking experiments with PPQ in the binding pocket comprising a β_2-Met^{286}Trp mutation. Based on photolabeling studies, the β_2-Met^{286} residue has previously been proposed to contribute to or line the etomidate binding site in the $\beta^{(+)}/\alpha^{(-)}$ TMD interface of GABA$_A$Rs,[19,31] and substitution of this Met^{286} for a Trp residue has been found to be detrimental to etomidate-mediated PAM activity and to also reduce the modulatory efficacies of MTQ and 2-phenyl-3-(*p*-tolyl)quinazolin-4(3*H*)-one at GABA$_A$Rs.[23,33,34] The docking of PPQ into $\beta_2^{(+)\text{Met286Trp}}/\alpha_1^{(-)}$ yielded seemingly reasonable modulator binding modes in the interface, and the binding modes of PPQ in wild-type $\beta_2^{(+)}/\alpha_1^{(-)}$ and in $\beta_2^{(+)\text{Met286Trp}}/\alpha_1^{(-)}$ are superimposed in Figure 5. It can be clearly seen that in the $\beta_2^{(+)\text{Met286Trp}}/\alpha_1^{(-)}$ TMD interface, PPQ is prevented from binding deeper into the binding pocket, and thus it does not reach the β_2-TM2/α_1-TM2 helices. While this deeper intrusion into the binding pocket potentially could be important for the PAM activity exhibited by this modulator class, it cannot be ruled out that the β_2-Met^{286}Trp mutation simply blocks the entrance of the modulator into the binding pocket.

Binding Mode of Cl-PPQ in the $\beta_2^{(+)}/\alpha_1^{(-)}$ TMD Interface. Docking of Cl-PPQ, a 5−12-fold more potent PAM than the PPQ analog at GABA$_A$Rs, into the $\beta_2^{(+)}/\alpha_1^{(-)}$ TMD interface also resulted in five binding modes, which are superimposed on the five binding modes of PPQ (Figure 6). This analysis revealed that the two modulators occupy the pocket in roughly the same manner, and thus the higher modulatory potency of Cl-PPQ is again likely due to increased steric bulk and lipophilicity of the ligand, rather than specific interactions with receptor residues or a more optimal binding mode.

https://dx.doi.org/10.1021/acschemneuro.0c00600
ACS Chem. Neurosci. XXXX, XXX, XXX−XXX

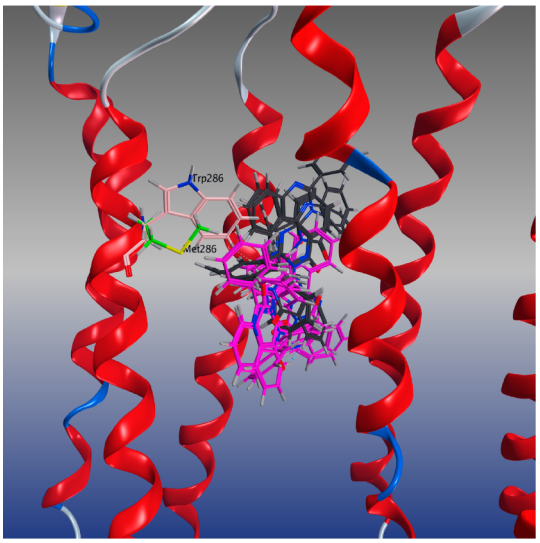

Figure 5. Superimposition of computationally determined plausible binding modes of PPQ in the wild-type $\beta_2^{(+)}/\alpha_1^{(-)}$ (black) and the $\beta_2^{(+)\text{Met286Trp}}/\alpha_1^{(-)}$ (purple) TMD interfaces. The β_2-Met^{286}Trp mutation prevents PPQ from binding deeper in the pocket, thus not reaching the β_2TM2/α_1TM2 helices.

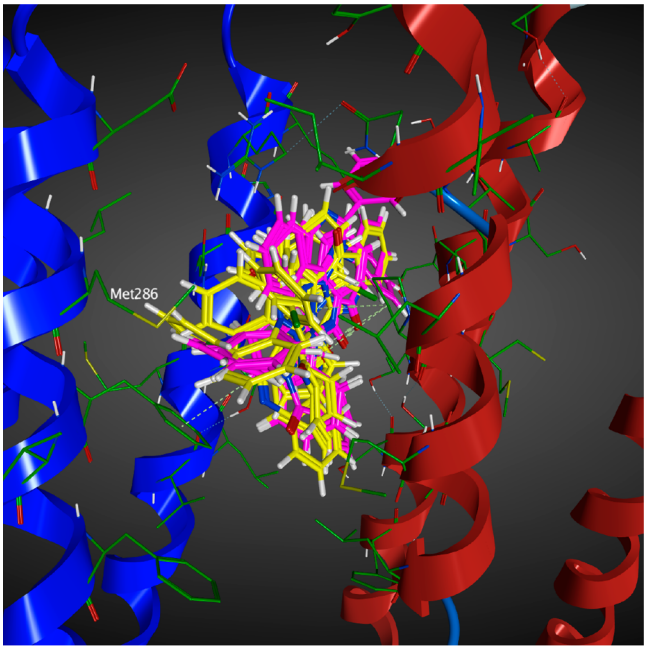

Figure 6. Superimposition of the *in silico* predicted five binding modes of Cl-PPQ (yellow) and the five binding modes of PPQ (purple).

CONCLUSION

In our previous search for novel GABA$_A$R PAMs based on the quinazolin-4(3*H*)-one scaffold, we exclusively focused on 2- and 3-substituents and identified a 2-aryl group and *ortho*-substituents on this ring as key contributors to high modulatory potency.[34] Although the investigations into the functional implications of 6-, 7-, and 8-substitutions to the quinazolin-4(3*H*)-one scaffold in the present work did not yield analogs with substantially improved modulatory potencies than that of the lead PPQ, some interesting SAR observations could be extracted from the study. While the introduction of even small 7-substituents was detrimental to PAM activity and only relatively small substituents could be accommodated in the 6-position of the quinazolin-4(3*H*)-one, the SAR for the 8-position was considerably more diverse. Notably, PPQ potency was retained in analogs comprising unbranched aliphatic substituents or selected heterocycles in the 8-position (**5l,o** and **6b,c**), and thus it may be possible to build further out from these substituents into regions in the $\beta^{(+)}/\alpha^{(-)}$ TMD interface not probed by the analogs in this study. Finally, after the elaborate delineation of the SAR of these GABA$_A$R PAMs performed in this and our previous study,[34] the 5-position remains the only unexplored position in the quinazolin-4(3*H*)-one scaffold, and it would be interesting to probe the impact of substituents in this position in future quinazolin-4(3*H*)-one analogs provided that a feasible synthetic route could be established.

The *in silico* study of MTQ and PPQ binding to the $\beta_2^{(+)}/\alpha_1^{(-)}$ TMD interface revealed a handful of putative binding modes for both PAMs. None of these could be excluded based on available mutagenesis data. The multiple putative binding modes are perhaps not surprising considering the lipophilic nature of the modulators and the residues lining this interface, but it obviously constitutes a challenge in terms of future structure-based modulator design for this binding site.

EXPERIMENTAL SECTION

Chemistry. All reactions involving dry solvents or sensitive agents were performed under a nitrogen atmosphere, and glassware was dried prior to use. Solvents were dried according to standard procedures, and reactions were monitored by analytical thin-layer chromatography (TLC, Merck silica gel 60 F_{254} aluminum sheets). Flash chromatography was carried out using Merck silica gel 60A (35−70 μm). ^{1}H and ^{13}C NMR spectra were recorded on a Bruker 400 MHz spectrometer (^{1}H NMR, 400 MHz; ^{13}C NMR, 100 MHz) or a Bruker 600 MHz spectrometer (^{1}H NMR, 600 MHz; ^{13}C NMR, 150 MHz). NMR data were obtained in $CDCl_3$ or DMSO-d_6 (purchased from Cambridge Isotope Laboratories, Inc.). MS spectra were recorded using a Waters Acquity UPLC-MS instrument with dual-wavelength detection with electrospray ionization. Gradients of 5% aqueous MeCN + 0.1% HCO_2H (solvent A) and 95% aqueous MeCN + 0.05% HCO_2H (solvent B) were employed. Analytical HPLC was performed using a Dionex UltiMate 3000 pump and photodiode array detector (200 and 210 nm, respectively) installed with an XTerra MS C_{18} 3.5 μm, 4.6 mm × 150 mm column, using a 5 → 95% MeCN gradient in H_2O containing 0.1% TFA. Optical rotation was measured using a PerkinElmer 241 polarimeter with Na lamp (589 nm). All commercial chemicals were used without further purification. The purity of all tested compounds was determined by HPLC to be >95%. The chemical structures of all final compounds synthesized were confirmed by ^{1}H NMR, ^{13}C NMR, and UPLC-MS.

Compound Synthesis. *General Procedure for the Synthesis of 2,3-Diphenylquinazolin-4-ones **4a**−**r**.* To a solution of anthranilic acid **1a**−**r** (0.4 mmol, 1 equiv) dissolved in dry DCM (15 mL) was added benzoyl chloride (0.42 mmol, 1.05 equiv), followed by the dropwise addition of TEA (0.6 mmol, 1.5 equiv) at 0 °C. The reaction mixture was warmed up to rt and stirred for 5 h before quenching with 1 × HCl solution (1 mL). The resulting precipitate was filtered, washed with heptane (3 × 10 mL), and dried under vacuum to afford the corresponding compounds **2a**−**r** (90−96%).

2-Benzoylamino-benzoic acid **2a**−**r** (0.36 mmol, 1 equiv) was dissolved in acetic anhydride (5.4 mmol, 15 equiv), and the solution was refluxed until starting material was consumed (TLC monitoring). Excess solvent was removed under vacuum, and heptane (20 mL) was added. The mixture was stirred vigorously for 30 min, filtered, washed with heptane (3 × 10 mL), and dried under vacuum to afford the compounds **3a**−**r** (84−92%).

https://dx.doi.org/10.1021/acschemneuro.0c00600
ACS Chem. Neurosci. XXXX, XXX, XXX−XXX

2-Phenyl-benzoxazin-4-one **3a**−**r** (0.3 mmol, 1 equiv) was dissolved in 10 mL of acetic acid, and aniline (0.315 mmol, 1.05 equiv) was added. The mixture was refluxed overnight before the solvent was removed under vacuum. The resulting solid was partitioned between CH_2Cl_2 (20 mL) and water (20 mL), and then the aqueous layer was extracted with CH_2Cl_2 (3 × 20 mL). The combined organic layers were washed with brine (20 mL), dried over Na_2SO_4, filtered, and concentrated under vacuum. The crude residue was purified by flash chromatography on silica gel (heptane−EtOAc 6:1, isocratic) to afford the title compounds **4a**−**r** (35−86%).

*6-Chloro-2,3-diphenylquinazolin-4(3H)-one (**4a**).* White solid, yield 24%. ^{1}H NMR (400 MHz, DMSO-d_6) δ 8.15 (dd, J = 5.9, 2.7 Hz, 1H), 7.95 (dt, J = 7.8, 3.9 Hz, 1H), 7.81 (dd, J = 9.1, 5.7 Hz, 1H), 7.70−7.07 (m, 10H) ppm. ^{13}C NMR (101 MHz, DMSO-d_6) δ 155.61, 146.38, 137.92, 137.41, 129.72, 129.60, 129.51, 129.08, 129.01, 128.95, 128.61, 128.04, 120.81 ppm. MS (ESI+) m/z: 333.1 $[M + H]^+$.

*7-Chloro-2,3-diphenylquinazolin-4(3H)-one (**4b**).* White solid, yield 69%. ^{1}H NMR (400 MHz, chloroform-d) δ 8.21 (dd, J = 8.5, 2.4 Hz, 1H), 7.75 (d, J = 2.1 Hz, 1H), 7.41 (dd, J = 8.6, 2.1 Hz, 1H), 7.35−7.03 (m, 10H) ppm. ^{13}C NMR (101 MHz, chloroform-d) δ 161.70, 156.46, 148.48, 140.95, 137.42, 135.14, 129.56, 129.06, 129.04, 128.98, 128.71, 128.59, 128.04, 127.87, 127.34, 119.45 ppm. MS (ESI+) m/z: 333.1 $[M + H]^+$.

*8-Chloro-2,3-diphenylquinazolin-4(3H)-one (**4c**).* White solid, yield 43%. ^{1}H NMR (400 MHz, chloroform-d) δ 8.19 (dd, J = 8.0, 1.5 Hz, 1H), 7.81 (dd, J = 7.7, 1.5 Hz, 1H), 7.42−7.04 (m, 11H) ppm. ^{13}C NMR (101 MHz, chloroform-d) δ 161.90, 155.62, 144.33, 137.57, 135.14, 134.96, 132.30, 129.64, 129.50, 129.05, 129.02, 128.58, 127.95, 127.20, 126.03, 122.58 ppm. MS (ESI+) m/z: 333.1 $[M + H]^+$.

*6,8-Dichloro-2,3-diphenylquinazolin-4(3H)-one (**4d**).* White solid, yield 55%. ^{1}H NMR (400 MHz, chloroform-d) δ 8.16 (d, J = 2.4 Hz, 1H), 7.80 (d, J = 2.4 Hz, 1H), 7.33−7.20 (m, 6H), 7.14 (dd, J = 8.2, 6.6 Hz, 2H), 7.09−7.04 (m, 2H) ppm. ^{13}C NMR (101 MHz, chloroform-d) δ 134.96, 132.53, 129.82, 129.46, 129.14, 128.90, 128.76, 128.00, 125.44, 123.10 ppm. MS (ESI+) m/z: 367.0 $[M + H]^+$.

*7,8-Dichloro-2,3-diphenylquinazolin-4(3H)-one (**4e**).* White solid, yield 61%. ^{1}H NMR (400 MHz, chloroform-d) δ 8.12 (dt, J = 8.4, 2.2 Hz, 1H), 7.69−7.04 (m, 11H) ppm. ^{13}C NMR (101 MHz, chloroform-d) δ 129.86, 129.50, 129.11, 128.93, 128.72, 128.38, 128.00, 125.94 ppm. MS (ESI+) m/z: 367.0 $[M + H]^+$.

*2,3-Diphenyl-7-(trifluoromethyl)quinazolin-4(3H)-one (**4f**).* White solid, yield 42%. ^{1}H NMR (400 MHz, chloroform-d) δ 8.40 (d, J = 8.3 Hz, 1H), 8.05 (d, J = 1.7 Hz, 1H), 7.66 (dd, J = 8.3, 1.7 Hz, 1H), 7.35−7.04 (m, 10H) ppm. ^{13}C NMR (101 MHz, chloroform-d) δ 161.54, 156.58, 147.52, 137.28, 134.96, 129.70, 129.14, 128.98, 128.96, 128.72, 128.41, 128.08, 125.38, 125.34, 123.31, 123.22, 123.18 ppm. MS (ESI+) m/z: 367.1 $[M + H]^+$.

*6-Bromo-2,3-diphenylquinazolin-4(3H)-one (**4g**).* White solid, yield 45%. ^{1}H NMR (400 MHz, chloroform-d) δ 8.41 (d, J = 2.3 Hz, 1H), 7.82 (dd, J = 8.7, 2.3 Hz, 1H), 7.62 (d, J = 8.6 Hz, 1H), 7.28−7.12 (m, 8H), 7.11−7.04 (m, 2H) ppm. ^{13}C NMR (101 MHz, chloroform-d) δ 137.92, 129.72, 129.60, 129.51, 129.08, 129.01, 128.95, 128.61, 128.04, 120.81 ppm. MS (ESI+) m/z: 368.1 $[M + H]^+$.

*6-Methoxy-2,3-diphenylquinazolin-4(3H)-one (**4h**).* White solid, yield 55%. ^{1}H NMR (400 MHz, chloroform-d) δ 7.72−7.63 (m, 2H), 7.34 (dd, J = 8.9, 2.9 Hz, 1H), 7.27−7.06 (m, 10H), 3.87 (s, 3H) ppm. ^{13}C NMR (101 MHz, chloroform-d) δ 158.83, 153.04, 142.14, 137.85, 135.53, 129.38, 129.13, 129.10, 129.03, 128.94, 128.36, 127.96, 124.87, 121.78, 106.64, 55.89 ppm. MS (ESI+) m/z: 329.1 $[M + H]^+$.

*6,7-Dimethoxy-2,3-diphenylquinazolin-4(3H)-one (**4i**).* White solid, yield 39%. ^{1}H NMR (400 MHz, chloroform-d) δ 7.61 (d, J = 6.2 Hz, 1H), 7.34−7.05 (m, 11H), 4.14−3.85 (m, 6H) ppm. ^{13}C NMR (101 MHz, chloroform-d) δ 161.61, 155.30, 154.12, 149.47, 143.76, 137.86, 135.61, 129.18, 129.11, 128.95, 128.90, 128.32, 127.97, 114.27, 108.24, 106.10, 56.38 ppm. MS (ESI+) m/z: 359.2 $[M + H]^+$.

*2,3-Diphenyl-6-(p-tolyl)quinazolin-4(3H)-one (**4j**).* White solid, yield 52%. ^{1}H NMR (400 MHz, chloroform-d) δ 8.49 (d, J = 2.2 Hz, 1H), 7.99 (dd, J = 8.4, 2.1 Hz, 1H), 7.81 (d, J = 8.5 Hz, 1H), 7.55 (d, J = 7.8 Hz, 2H), 7.31−7.09 (m, 12H), 2.35 (s, 3H) ppm. ^{13}C NMR (101 MHz, chloroform-d) δ 146.51, 140.18, 137.86, 137.76, 136.77, 135.51, 133.50, 129.76, 129.29, 129.15, 129.03, 128.99, 128.42, 128.23, 128.00, 127.06, 124.72, 121.21, 21.15 ppm. MS (ESI+) m/z: 389.2 $[M + H]^+$.

*2,3-Diphenyl-6-(4-(trifluoromethyl)phenyl)quinazolin-4(3H)-one (**4k**).* White solid, yield 53%. ^{1}H NMR (400 MHz, chloroform-d) δ 8.53 (dd, J = 7.9, 4.7 Hz, 1H), 8.11−7.65 (m, 6H), 7.47−7.04 (m, 10H) ppm. ^{13}C NMR (101 MHz, chloroform-d) δ 133.53, 129.46, 129.09, 129.06, 129.01, 128.62, 128.56, 128.05, 127.52, 125.55, 121.36 ppm. MS (ESI+) m/z: 443.1 $[M + H]^+$.

*6-Nitro-2,3-diphenylquinazolin-4(3H)-one (**4l**).* Yellow solid, yield 30%. ^{1}H NMR (400 MHz, chloroform-d) δ 9.13 (s, 1H), 8.52 (dd, J = 8.9, 2.7 Hz, 1H), 7.86 (d, J = 8.9 Hz, 1H), 7.30−7.08 (m, 10H) ppm. ^{13}C NMR (101 MHz, chloroform-d) δ 161.20, 158.41, 151.53, 145.98, 136.95, 134.67, 130.09, 129.36, 129.25, 129.02, 128.96, 128.87, 128.78, 128.17, 123.92, 121.15 ppm. MS (ESI+) m/z: 344.1 $[M + H]^+$.

*8-Nitro-2,3-diphenylquinazolin-4(3H)-one (**4m**).* Yellow solid, yield 29%. ^{1}H NMR (400 MHz, chloroform-d) δ 8.59 (d, J = 2.2 Hz, 1H), 8.44 (d, J = 8.7 Hz, 1H), 8.21 (dd, J = 8.7, 2.2 Hz, 1H), 7.29−7.16 (m, 8H), 7.13−7.07 (m, 2H) ppm. ^{13}C NMR (101 MHz, chloroform-d) δ 161.17, 157.37, 151.91, 148.09, 137.06, 134.66, 129.94, 129.22, 129.19, 129.01, 128.90, 128.86, 128.14, 125.10, 123.39, 120.83 ppm. MS (ESI+) m/z: 344.1 $[M + H]^+$.

*4-Oxo-2,3-diphenyl-3,4-dihydroquinazolin-6-yl Benzoate (**4n**).* White solid, yield 68%. ^{1}H NMR (400 MHz, chloroform-d) δ 8.21 (d, J = 7.7 Hz, 2H), 7.62−7.53 (m, 2H), 7.46 (dt, J = 19.3, 7.8 Hz, 3H), 7.28−7.15 (m, 6H), 7.13−7.04 (m, 3H), 6.99 (t, J = 7.6 Hz, 2H) ppm. ^{13}C NMR (101 MHz, chloroform-d) δ 165.30, 161.96, 154.87, 146.95, 137.72, 135.16, 133.54, 130.40, 129.57, 129.47, 129.35, 129.08, 128.98, 128.52, 128.47, 127.57, 127.37, 127.05, 125.02 ppm. MS (ESI+) m/z: 419.2 $[M + H]^+$.

*4-Oxo-2,3-diphenyl-3,4-dihydroquinazolin-8-yl Benzoate (**4o**).* White solid, yield 59%. ^{1}H NMR (400 MHz, DMSO-d_6) δ 8.17 (d, J = 7.8 Hz, 3H), 7.88 (d, J = 7.8 Hz, 1H), 7.75 (t, J = 7.4 Hz, 1H), 7.68 (t, J = 7.9 Hz, 1H), 7.61 (t, J = 7.7 Hz, 2H), 7.38−7.08 (m, 10H) ppm. ^{13}C NMR (101 MHz, DMSO-d_6) δ 130.31, 129.92, 129.49, 129.44, 129.09, 128.77, 127.93, 127.71, 124.79 ppm. MS (ESI+) m/z: 419.2 $[M + H]^+$.

*8-Bromo-2,3-diphenylquinazolin-4(3H)-one (**4p**).* White solid, yield 76%. ^{1}H NMR (400 MHz, DMSO-d_6) δ 8.22 (m, 2H), 7.51 (t, J = 7.8 Hz, 1H), 7.44−7.39 (m, 2H), 7.39−7.20 (m, 8H)) ppm. ^{13}C NMR (101 MHz, DMSO-d_6) δ 161.45, 138.56, 138.12, 135.92, 129.87, 129.57, 129.48, 129.06, 128.79, 128.42, 127.99, 126.81, 122.99, 122.55 ppm. MS (ESI+) m/z: 368.1 $[M + H]^+$.

*8-Fluoro-2,3-diphenylquinazolin-4(3H)-one (**4q**).* White solid, yield 61%. ^{1}H NMR (400 MHz, DMSO-d_6) δ 8.03 (dd, J = 8.0, 1.3 Hz, 1H), 7.80 (ddd, J = 10.7, 8.1, 1.4 Hz, 1H), 7.60 (td, J = 8.0, 4.8 Hz, 1H), 7.42−7.20 (m, 10H) ppm. ^{13}C NMR (101 MHz, DMSO-d_6) δ 156.34, 138.10, 135.92, 129.89, 129.52, 129.39, 129.06, 128.77, 127.98, 127.89, 123.35, 122.71, 120.70, 120.51 ppm. MS (ESI+) m/z: 317.1 $[M + H]^+$.

*8-Methoxy-2,3-diphenylquinazolin-4(3H)-one (**4r**).* White solid, yield 37%. ^{1}H NMR (400 MHz, DMSO-d_6) δ 7.79−7.72 (m, 1H), 7.55 (td, J = 8.0, 2.5 Hz, 1H), 7.46 (d, J = 8.0 Hz, 1H), 7.37 (dt, J = 7.9, 2.2 Hz, 2H), 7.35−7.17 (m, 8H), 3.95 (d, J = 2.4 Hz, 3H) ppm. ^{13}C NMR (101 MHz, DMSO) δ 155.18, 154.29, 138.32, 136.26, 129.92, 129.43, 129.23, 129.02, 128.61, 128.01, 127.91, 122.28, 117.84, 115.76, 56.47 ppm. MS (ESI+) m/z: 329.1 $[M + H]^+$.

*General Procedure for the Synthesis of **5a** and **5b**.* A solution of KOH (0.38 mmol, 2 equiv) in 4 mL of H_2O was added dropwise to **4l** or **4m** (0.19 mmol, 1 equiv) in 1 mL of ethanol. The mixture was heated at 60 °C for 5 h, cooled to rt, and quenched with dilute 1 × HCl solution (1 mL). Afterward, the solvent was removed under

https://dx.doi.org/10.1021/acschemneuro.0c00600
ACS Chem. Neurosci. XXXX, XXX, XXX−XXX

vacuum. The crude residue was purified by flash chromatography on silica gel (heptane−EtOAc 1:1, isocratic) to afford the title compound **5a** or **5b**.

*6-Hydroxy-2,3-diphenylquinazolin-4(3H)-one (**5a**).* White solid, yield 19%. ^{1}H NMR (400 MHz, DMSO-d_6) δ 10.17 (s, 1H), 7.65 (d, J = 8.8 Hz, 1H), 7.50 (d, J = 2.8 Hz, 1H), 7.39−7.15 (m, 11H) ppm. ^{13}C NMR (101 MHz, DMSO-d_6) δ 148.88, 138.05, 135.79, 130.64, 130.12, 129.89, 129.53, 129.40, 129.34, 129.06, 128.76, 127.98, 120.40 ppm. MS (ESI+) m/z: 315.1 $[M + H]^+$.

*8-Hydroxy-2,3-diphenylquinazolin-4(3H)-one (**5b**).* White solid, yield 23%. ^{1}H NMR (400 MHz, DMSO-d_6) δ 9.76 (s, 1H), 7.63 (dd, J = 7.9, 1.4 Hz, 1H), 7.42 (ddd, J = 7.8, 4.9, 3.1 Hz, 3H), 7.36−7.16 (m, 9H) ppm. ^{13}C NMR (101 MHz, DMSO-d_6) δ 153.83, 153.61, 138.43, 136.80, 136.13, 130.00, 129.65, 129.24, 128.99, 128.56, 128.18, 127.87, 122.13, 119.36, 116.66 ppm. MS (ESI+) m/z: 315.1 $[M + H]^+$.

*General Procedure for the Synthesis of Suzuki Coupling Products **5c**−**h**.* In an inert atmosphere of Ar, to a microwave vial was added **4p** (0.3 mmol, 1 equiv), borate (0.33 mmol, 1.1 equiv), $Pd(PPh_3)_4$ (0.015 mmol, 5 mol %), Cs_2CO_3 (0.6 mmol, 3 equiv), and 2 mL of toluene. The vial was capped and heated at 100 °C overnight. The resulting solid was partitioned between EtOAc (20 mL) and water (20 mL) and then the aqueous layer was extracted with EtOAc (3 × 20 mL). The combined organic layers were washed with brine (30 mL), dried over Na_2SO_4, filtered, and concentrated under vacuum. The crude residue was purified by flash chromatography on silica gel (heptane−EtOAc 6:1, isocratic) to afford the title compounds **5c**−**h** (43−78%).

*8-Methyl-2,3-diphenylquinazolin-4(3H)-one (**5c**).* White solid, yield 43%. ^{1}H NMR (400 MHz, DMSO-d_6): δ 8.05 (dd, J = 8.0, 1.5 Hz, 1H), 7.78 (d, J = 7.3 Hz, 1H), 7.50 (t, J = 7.6 Hz, 1H), 7.43−7.37 (m, 2H), 7.36−7.18 (m, 8H), 2.59 (s, 3H)) ppm. ^{13}C NMR (101 MHz, DMSO-d_6) δ 129.98, 129.36, 129.02, 127.95, 126.94 ppm. MS (ESI+) m/z: 313.1 $[M + H]^+$.

*2,3-Diphenyl-8-(thiophen-3-yl)quinazolin-4(3H)-one (**5d**).* White solid, yield 78%. ^{1}H NMR (400 MHz, DMSO-d_6): δ 8.24−8.10 (m, 3H), 7.78 (d, J = 5.0 Hz, 1H), 7.68−7.58 (m, 2H), 7.46−7.40 (m, 2H), 7.40−7.18 (m, 8H) ppm. ^{13}C NMR (101 MHz, DMSO-d_6): δ 162.01, 138.61, 138.28, 136.30, 134.79, 133.35, 129.93, 129.91, 129.49, 129.41, 129.05, 128.64, 128.07, 127.58, 126.04, 125.79, 125.57, 122.06 ppm. MS (ESI+) m/z: 381.1 $[M + H]^+$.

*2,3-Diphenyl-8-(pyrimidin-5-yl)quinazolin-4(3H)-one (**5e**).* White solid, yield 67%. ^{1}H NMR (400 MHz, DMSO-d_6): δ 9.18 (d, J = 7.1 Hz, 3H), 8.34 (dd, J = 8.0, 1.5 Hz, 1H), 8.15 (dd, J = 7.5, 1.5 Hz, 1H), 7.76 (t, J = 7.7 Hz, 1H), 7.41−7.27 (m, 7H), 7.25−7.18 (m, 3H) ppm. ^{13}C NMR (101 MHz, DMSO-d_6): δ 157.88, 157.45, 138.16, 136.05, 135.78, 132.24, 129.85, 129.54, 129.39, 129.10, 128.75, 128.03, 127.80, 121.93 ppm. MS (ESI+) m/z: 377.2 $[M + H]^+$.

*8-(2-Methoxypyrimidin-5-yl)-2,3-diphenylquinazolin-4(3H)-one (**5f**).* White solid, yield 73%. ^{1}H NMR (400 MHz, DMSO-d_6): δ 9.00 (d, J = 1.2 Hz, 2H), 8.29 (d, J = 7.9 Hz, 1H), 8.09 (d, J = 7.4 Hz, 1H), 7.73 (t, J = 7.7 Hz, 1H), 7.43−7.22 (m, 9H), 3.97 (s, 3H) ppm. ^{13}C NMR (101 MHz, DMSO-d_6): δ 160.38, 144.71, 136.13, 135.24, 129.86, 129.49, 129.39, 129.09, 128.72, 128.05, 127.76, 127.28, 125.76, 55.18 ppm. MS (ESI+) m/z: 407.2 $[M + H]^+$.

*2,3-Diphenyl-8-propylquinazolin-4(3H)-one (**5g**).* White solid, yield 51%. ^{1}H NMR (400 MHz, DMSO-d_6) δ 8.06 (dd, J = 8.0, 1.6 Hz, 1H), 7.75 (dd, J = 7.4, 1.5 Hz, 1H), 7.52 (t, J = 7.6 Hz, 1H), 7.39 (dd, J = 7.7, 2.0 Hz, 2H), 7.36−7.19 (m, 8H), 3.01 (t, J = 7.5 Hz, 2H), 1.73 (q, J = 7.4 Hz, 2H), 0.94 (t, J = 7.3 Hz, 3H) ppm. ^{13}C NMR (101 MHz, DMSO-d_6) δ 140.23, 138.41, 136.44, 134.96, 129.97, 129.49, 129.30, 129.00, 128.57, 128.00, 127.19, 124.68, 121.24, 32.78, 23.83, 14.38 ppm. MS (ESI+) m/z: 341.2 $[M + H]^+$.

*8-Isobutyl-2,3-diphenylquinazolin-4(3H)-one (**5h**).* White solid, yield 53%. ^{1}H NMR (400 MHz, DMSO-d_6) δ 8.07 (dd, J = 7.9, 1.6 Hz, 1H), 7.72 (dd, J = 7.4, 1.6 Hz, 1H), 7.52 (t, J = 7.6 Hz, 1H), 7.42−7.36 (m, 2H), 7.34−7.19 (m, 8H), 2.91 (d, J = 7.1 Hz, 2H), 2.11 (dq, J = 13.5, 6.8 Hz, 1H), 0.91 (d, J = 6.6 Hz, 6H) ppm. ^{13}C NMR (101 MHz, DMSO-d_6) δ 162.16, 146.01, 139.40, 138.42, 136.46, 135.69, 129.96, 129.48, 129.32, 129.00, 128.56, 128.01, 127.02, 124.76, 121.23, 29.45, 22.92 ppm. MS (ESI+) m/z: 355.2 $[M + H]^+$.

*General Procedure for the Synthesis of Stille Coupling Products **5i**−**k**.* In an inert atmosphere of Ar, to a microwave vial was added **4p** (0.3 mmol, 1 equiv), tributyltin (0.45 mmol, 1.5 equiv), $Pd(PPh_3)_4$ (0.015 mmol, 5 mol %), and toluene (2 mL). The vial was capped and refluxed overnight. The reaction mixture was cooled to rt and stirred with an aqueous solution of saturated KF (10 mL) for an hour. The mixture was extracted with DCM (3 × 10 mL), and the combined organic layers were washed with brine (30 mL), dried over Na_2SO_4, filtered, and concentrated under vacuum. The crude residue was purified by flash chromatography on silica gel (heptane−EtOAc 6:1, isocratic) to afford the title compounds **5i**−**k** (31−55%).

*2,3-Diphenyl-8-vinylquinazolin-4(3H)-one (**5i**).* White solid, yield 53%. ^{1}H NMR (400 MHz, DMSO-d_6) δ 8.17 (ddd, J = 14.4, 7.8, 1.4 Hz, 2H), 7.74−7.58 (m, 2H), 7.46−7.19 (m, 10H), 6.07 (dd, J = 17.9, 1.4 Hz, 1H), 5.46 (dd, J = 11.1, 1.3 Hz, 1H) ppm. ^{13}C NMR (101 MHz, DMSO-d_6) δ 138.29, 131.93, 129.94, 129.47, 129.39, 129.03, 128.65, 128.00, 127.38, 126.56, 121.62, 116.99 ppm. MS (ESI+) m/z: 325.1 $[M + H]^+$.

*8-Allyl-2,3-diphenylquinazolin-4(3H)-one (**5j**).* White solid, yield 32%. ^{1}H NMR (400 MHz, DMSO-d_6) δ 8.09 (dd, J = 7.9, 1.5 Hz, 1H), 7.75 (dd, J = 7.4, 1.5 Hz, 1H), 7.54 (t, J = 7.6 Hz, 1H), 7.42−7.38 (m, 2H), 7.35−7.21 (m, 8H), 6.11 (m, 1H), 5.19−5.01 (m, 2H), 3.82 (d, J = 6.7 Hz, 2H) ppm. ^{13}C NMR (101 MHz, chloroform-d) δ 145.14, 137.99, 137.95, 134.94, 129.44, 129.17, 129.14, 128.91, 128.28, 127.73, 126.84, 125.36, 112.24, 38.32, 22.54 ppm. MS (ESI+) m/z: 339.2 $[M + H]^+$.

*8-(2-Methylallyl)-2,3-diphenylquinazolin-4(3H)-one (**5k**).* White solid, yield 56%. ^{1}H NMR (400 MHz, DMSO-d_6) δ 8.10 (dd, J = 7.9, 1.6 Hz, 1H), 7.73 (dd, J = 7.4, 1.6 Hz, 1H), 7.55 (t, J = 7.6 Hz, 1H), 7.44−7.19 (m, 10H), 4.84 (dd, J = 2.4, 1.4 Hz, 1H), 4.73 (dd, J = 2.5, 1.2 Hz, 1H), 3.79 (s, 2H), 1.72 (t, J = 1.1 Hz, 3H) ppm. ^{13}C NMR (101 MHz, DMSO-d_6) δ 162.10, 144.99, 138.38, 137.67, 135.23, 129.96, 129.52, 129.37, 129.02, 128.60, 127.99, 127.24, 125.14, 121.26, 112.75, 38.07, 22.88 ppm. MS (ESI+) m/z: 353.2 $[M + H]^+$.

*General Procedure for the Synthesis of **5l** and **5m**.* In an inert atmosphere of Ar, to a microwave vial containing P(t-Bu)$_3$ (0.02 mmol, 2% mol), $Pd_2(dba)_3$ (0.01 mmol, 1% mmol), and **4p** (1 mmol, 1 equiv) in DMF (1 mL) was added trimethylsilylacetonitrile (1.2 mmol, 1.2 equiv), followed by ZnF_2 (0.6 mmol, 0.6 equiv). The heterogeneous reaction mixture was stirred at 90 °C for 8 h. The crude reaction was then allowed to cool to room temperature and diluted with Et_2O (50 mL). The resulting solution was washed with H_2O. The organic phase was dried over Na_2SO_4, filtered, and concentrated at reduced pressure. The residue was then purified by chromatography on silica gel (heptane−EtOAc 10:1, isocratic) to afford the title compound **5l** (47%).

When the reaction was allowed to proceed for a longer time (>18 h), an unexpected Knoevenagel reaction occurred and gave the main product **5m** (79%).

*2-(4-Oxo-2,3-diphenyl-3,4-dihydroquinazolin-8-yl)acetonitrile (**5l**).* White solid, yield 48%. ^{1}H NMR (400 MHz, DMSO-d_6) δ 8.20 (d, J = 8.0 Hz, 1H), 7.98 (d, J = 7.4 Hz, 1H), 7.63 (td, J = 7.8, 2.0 Hz, 1H), 7.42 (d, J = 7.3 Hz, 2H), 7.39−7.20 (m, 8H), 4.33 (d, J = 2.9 Hz, 2H) ppm. ^{13}C NMR (101 MHz, DMSO-d_6) δ 161.70, 145.42, 138.14, 135.96, 134.91, 129.91, 129.63, 129.60, 129.09, 129.05, 128.77, 128.02, 127.58, 126.96, 121.45, 119.40, 19.26 ppm. MS (ESI +) m/z: 338.1 $[M + H]^+$.

*3-(Dimethylamino)-2-(4-oxo-2,3-diphenyl-3,4-dihydroquinazolin-8-yl)acrylonitrile (**5m**).* White solid, yield 80%. ^{1}H NMR (400 MHz, DMSO-d_6) δ 7.99 (dd, J = 7.9, 1.5 Hz, 1H), 7.84 (s, 1H), 7.77 (dd, J = 7.6, 1.5 Hz, 1H), 7.54 (t, J = 7.8 Hz, 1H), 7.49−7.44 (m, 2H), 7.35−7.22 (m, 8H), 3.20 (s, 6H) ppm. ^{13}C NMR (101 MHz, DMSO-d_6) δ 162.06, 155.97, 153.69, 138.25, 136.19, 135.06, 132.69, 129.85, 129.70, 129.54, 129.08, 128.64, 128.00, 127.49, 123.61, 121.91, 70.88 ppm. MS (ESI+) m/z: 394.2 $[M + H]^+$.

*8-Acetyl-2,3-diphenylquinazolin-4(3H)-one (**5n**).* A microwave vial was charged with 1,3,5-trimethoxybenzene (0.03 mmol, 0.1

https://dx.doi.org/10.1021/acschemneuro.0c00600
ACS Chem. Neurosci. XXXX, XXX, XXX−XXX

equiv), and **4p** (0.3 mmol, 1 equiv), CsF (1.2 mmol, 1 equiv), and $Pd(PPh_3)_4$ (0.03 mmol, 10% mol) were added to the vial. The vial was placed under an atmosphere of Ar and 1,2-dichloroethane (0.5 mL) and acetyltrimethylsilane (0.6 mmol, 2 equiv) were added. The vial was capped and heated to 75 °C for 6 h. After cooling to rt, the mixture was diluted with heptane (0.5 mL) and filtered through a plug of silica gel (10 mL EtOAc eluent), and the volatiles removed under reduced pressure. The crude residue was purified by flash chromatography on silica gel (heptane−EtOAc 3:1, isocratic) to afford the title compound **5n** (27%). White solid, yield 27.8%. ^{1}H NMR (400 MHz, DMSO-d_6) δ 8.37 (dt, J = 7.9, 1.4 Hz, 1H), 8.03 (dt, J = 7.5, 1.5 Hz, 1H), 7.72−7.63 (m, 1H), 7.42 (dt, J = 7.7, 1.4 Hz, 2H), 7.41−7.21 (m, 8H), 2.79 (s, 3H) ppm. ^{13}C NMR (101 MHz, DMSO-d_6) δ 134.18, 130.20, 129.88, 129.67, 129.46, 129.09, 128.79, 128.10, 99.98, 32.92 ppm. MS (ESI+) m/z: 341.1 $[M + H]^+$.

*8-Morpholino-2,3-diphenylquinazolin-4(3H)-one (**5o**).* A solution of **4p** (0.3 mmol, 1 equiv) in toluene (1 mL) was added to a mixture of morpholine (0.3 mmol, 1 equiv), $Pd_2(dba)_3$ (7.5 μmol, 2.5 mol %), Xantphos (15 μmol, 5 mol %), and Cs_2CO_3 (0.36 mmol, 1.2 equiv) under an atmosphere of Ar. The reaction mixture was heated at 100 °C for 4 h, and then the cooled reaction mixture was diluted with ethyl acetate and filtered through Celite, and the filtrate was concentrated under vacuum. The resultant residue was subjected to flash chromatography (heptane−EtOAc 3:1, isocratic) to give the title compound **5o** as a white solid, yield 63%. ^{1}H NMR (400 MHz, DMSO-d_6): δ 7.79 (dd, J = 7.9, 1.3 Hz, 1H), 7.49 (t, J = 7.9 Hz, 1H), 7.39 (dd, J = 7.8, 1.8 Hz, 2H), 7.36−7.22 (m, 9H), 3.77 (t, J = 4.6 Hz, 4H), 3.35 (dd, J = 5.9, 3.3 Hz, 4H) ppm. ^{13}C NMR (101 MHz, DMSO-d_6) δ 162.18, 152.65, 148.44, 140.48, 138.38, 136.38, 129.88, 129.49, 129.39, 129.02, 128.57, 128.02, 127.90, 122.38, 121.95, 119.19, 66.67, 52.00 ppm. MS (ESI+) m/z: 384.2 $[M + H]^+$.

*2-(4-Oxo-2,3-diphenyl-3,4-dihydroquinazolin-8-yl)acetic Acid (**6a**).* Compound **5l** (0.3 mmol, 1 equiv) was treated with KOH (0.39 mmol, 1.3 equiv) in 4 mL of water. The mixture was heated at 60 °C for 5 h, cooled to rt, and quenched with dilute 1 × HCl solution (1 mL). The solvent was removed under vacuum, and the crude residue was purified by flash chromatography on silica gel (heptane−EtOAc 1:1, isocratic) to afford the title compound **6a** as a white solid, yield 8.1%. ^{1}H NMR (400 MHz, DMSO-d_6) δ 12.27 (s, 1H), 8.12 (dd, J = 8.0, 1.5 Hz, 1H), 7.83 (dd, J = 7.4, 1.5 Hz, 1H), 7.56 (t, J = 7.7 Hz, 1H), 7.44−7.18 (m, 10H), 4.01 (s, 2H) ppm. ^{13}C NMR (101 MHz, DMSO-d_6) δ 172.94, 161.95, 146.07, 136.45, 136.15, 133.62, 129.94, 129.58, 129.47, 129.06, 128.67, 128.0, 127.17, 125.72, 121.07, 36.42 ppm. MS (ESI+) m/z: 357.1 $[M + H]^+$.

*8-(5-Aminoisoxazol-4-yl)-2,3-diphenylquinazolin-4(3H)-one (**6b**).* To a microwave vial containing **5m** (0.2 mmol, 1 equiv) and hydroxylamine hydrochloride (0.3 mmol, 1.5 equiv) was added EtOH (3 mL). The vial was capped and refluxed for 1 h. The solvent was removed under vacuum, and the crude residue was purified by flash chromatography on silica gel (heptane−EtOAc 3:1, isocratic) to afford the title compound **6b** as a white solid, yield 41%. ^{1}H NMR (400 MHz, DMSO-d_6) δ 8.64 (s, 1H), 8.08 (d, J = 7.8 Hz, 1H), 7.94 (d, J = 7.5 Hz, 1H), 7.60 (t, J = 7.7 Hz, 1H), 7.51−7.42 (m, 2H), 7.41−7.12 (m, 10H) ppm. ^{13}C NMR (101 MHz, DMSO-d_6) δ 166.91, 162.04, 154.65, 153.08, 143.72, 136.05, 133.47, 129.87, 129.47, 129.35, 129.04, 128.64, 128.09, 127.61, 124.28, 122.00, 90.41 ppm. MS (ESI+) m/z: 381.1 $[M + H]^+$.

*8-(2-Oxopropyl)-2,3-diphenylquinazolin-4(3H)-one (**6c**).* To a solution of **5k** (0.2 mmol, 1 equiv) in a mixture of dry THF (3 mL)/deionized H_2O (2 mL) was added 4% OsO_4 in deionized H_2O (100 μL). The resulting mixture was stirred at rt for 20 min, and then $NaIO_4$ (0.9 mmol, 4.5 equiv) was added in several portions. The reaction mixture was stirred at rt for 16 h and then quenched by the addition of saturated aqueous Na_2SO_3 solution (5 mL). The resulting mixture was extracted with ethyl acetate (2 × 10 mL), and the combined organic layers were washed with saturated aqueous $NaHCO_3$ solution (5 mL) and dried over Na_2SO_4, and the solvent was removed under reduced pressure. The resultant residue was subjected to flash chromatography (heptane−EtOAc 3:1, isocratic) to give the title compound **6c**, white solid, yield 63%. ^{1}H NMR (400 MHz, DMSO-d_6) δ 8.12 (dd, J = 8.0, 1.6 Hz, 1H), 7.76 (dd, J = 7.4, 1.6 Hz, 1H), 7.55 (t, J = 7.6 Hz, 1H), 7.39−7.20 (m, 10H), 4.15 (s, 2H), 2.19 (s, 3H) ppm. ^{13}C NMR (101 MHz, DMSO-d_6) δ 206.19, 136.61, 134.12, 129.93, 129.48, 129.05, 128.01, 127.21, 45.40, 30.59 ppm. MS (ESI+) m/z: 355.1 $[M + H]^+$.

Computational Study. For all computational work, the software package MOE 2019.01 was used. The crystal structure of the $\alpha_1\beta_2\gamma_2$ $GABA_AR$ (PDB code 6D6U)[39] was prepared by applying the algorithm Protonate3D (standard setup). Thereafter, chain A (β_2 subunit) and chain B (α_1 subunit) were extracted from the pentameric receptor complex. The SiteFinder algorithm was applied to identify the pocket formed at the intersection of β_2 TM2+TM3 and α_1 TM1+TM2. Docking was thereafter performed using the function Dock with standard parameter setup and REFINEMENT set to *Induced Fit*.

Pharmacology. The functional properties of the 36 PPQ analogs were characterized at human $\alpha_1\beta_2\gamma_{2S}$, $\alpha_3\beta_2\gamma_{2S}$, $\alpha_4\beta_2\gamma_{2S}$, $\alpha_5\beta_2\gamma_{2S}$, and $\alpha_6\beta_2\gamma_{2S}$ $GABA_ARs$ transiently expressed in tsA201 cells in the FLIPR Membrane Potential Blue (FMP) assay (Molecular Devices, Crawley, UK) essentially as previously described.[34] Briefly, tsA201 cells were cultured in Dulbecco's modified Eagle medium Glutamax-I supplemented with 10% fetal bovine serum, 100 U/mL penicillin, and 100 μg/mL streptomycin at 37 °C in a humidified 5% CO_2 atmosphere. Cells (2×10^6) were split into a 10 cm tissue culture plate and transfected the following day with a total of 8 μg of cDNA (2 μg of α-pCDNA3.1 (α_1, α_3, α_4, α_5, α_6), 2 μg β_2-pCDNA3.1, and 4 μg γ_{2S}-pCDNA3.1) using the Polyfect transfection reagent (Qiagen, Hilden, Germany). Sixteen to twenty hours after the transfection, the cells were split into poly(D-lysine)-coated black 96-well plates with clear bottoms (BD Biosciences, Palo Alto, CA). The following day, the culture medium was aspirated, and the cells were washed once with 100 μL of assay buffer (140 mM NaCl, 4.7 mM KCl, 2.5 mM $CaCl_2$, 1.2 mM $MgCl_2$, 11 mM HEPES, 10 mM D-glucose, pH 7.4), after which the cells were incubated in 100 μL of assay buffer supplemented with FMP dye (0.5 mg/mL) at 37 °C for 30 min. The 96-well plate was assayed in a FLEXStation[3] Benchtop Multi-Mode Microplate Reader (Molecular Devices, Crawley, U.K.) measuring emission [in fluorescence units (FU)] at 565 nm caused by excitation at 525 nm before and up to 90 s after addition of 33.3 μL of assay buffer supplemented with GABA (an EC_{10} assay concentration for the specific receptor subtype, determined on the day of the experiment) and various concentrations of the test compounds.

AUTHOR INFORMATION

Corresponding Authors

Anders A. Jensen − *Department of Drug Design and Pharmacology, Faculty of Health and Medical Sciences, University of Copenhagen, Copenhagen 2100, Denmark*; Phone: +45 23 96 24 34; Email: aaj@sund.ku.dk

Lennart Bunch − *Department of Drug Design and Pharmacology, Faculty of Health and Medical Sciences, University of Copenhagen, Copenhagen 2100, Denmark*; orcid.org/0000-0002-0180-4639; Phone: +45 35 33 62 44; Email: lebu@sund.ku.dk

Author

Peng-Fei Wang − *Department of Drug Design and Pharmacology, Faculty of Health and Medical Sciences, University of Copenhagen, Copenhagen 2100, Denmark; School of Pharmaceutical Sciences and Innovative Drug Research Centre, Chongqing University, Chongqing 400044, P.R. China*

Complete contact information is available at: https://pubs.acs.org/10.1021/acschemneuro.0c00600

https://dx.doi.org/10.1021/acschemneuro.0c00600
ACS Chem. Neurosci. XXXX, XXX, XXX−XXX

Author Contributions

The manuscript was written through contributions of all authors. All authors have given approval to the final version of the manuscript.

Notes

The authors declare no competing financial interest.

■ ACKNOWLEDGMENTS

The authors thank the International Postdoctoral Exchange Fellowship Program 2017 of China (No. 20170090) and the Novo Nordisk Foundation for financial support.

■ LIST OF ABBREVIATIONS

Cl-PPQ, 3-(2-chlorophenyl)-2-phenylquinazolin-4(3*H*)-one; FMP, FLIPR Membrane Potential; MTQ, methaqualone (2-methyl-3-(*o*-tolyl)-quinazolin-4(3*H*)-one); PAM, positive allosteric modulator; PPQ, 2,3-diphenylquinazolin-4(3*H*)-one

■ REFERENCES

(1) Olsen, R. W., and Sieghart, W. (2008) International Union of Pharmacology. LXX. Subtypes of γ-aminobutyric acid$_A$ receptors: classification on the basis of subunit composition, pharmacology, and function. Update. *Pharmacol. Rev. 60*, 243−60.

(2) Chua, H. C., and Chebib, M. (2017) GABA$_A$ Receptors and the Diversity in their Structure and Pharmacology. *Adv. Pharmacol. 79*, 1−34.

(3) Miller, P. S., and Aricescu, A. R. (2014) Crystal structure of a human GABA$_A$ receptor. *Nature 512*, 270−275.

(4) Laverty, D., Desai, R., Uchanski, T., Masiulis, S., Stec, W. J., Malinauskas, T., Zivanov, J., Pardon, E., Steyaert, J., Miller, K. W., and Aricescu, A. R. (2019) Cryo-EM structure of the human α1β3γ2 GABA$_A$ receptor in a lipid bilayer. *Nature 565* (7740), 516−520.

(5) Whiting, P. J. (2003) GABA-A receptor subtypes in the brain: a paradigm for CNS drug discovery? *Drug Discovery Today 8*, 445−50.

(6) Hörtnagl, H., Tasan, R. O., Wieselthaler, A., Kirchmair, E., Sieghart, W., and Sperk, G. (2013) Patterns of mRNA and protein expression for 12 GABA$_A$ receptor subunits in the mouse brain. *Neuroscience 236*, 345−72.

(7) Atack, J. R. (2011) GABA$_A$ receptor subtype-selective modulators. I. α2/α3-selective agonists as non-sedating anxiolytics. *Curr. Top. Med. Chem. 11*, 1176−1202.

(8) Stephens, D. N., King, S. L., Lambert, J. J., Belelli, D., and Duka, T. (2017) GABA$_A$ receptor subtype involvement in addictive behaviour. *Genes Brain Behav. 16*, 149−184.

(9) Atack, J. R. (2011) GABA$_A$ receptor subtype-selective modulators. II. α5-selective inverse agonists for cognition enhancement. *Curr. Top. Med. Chem. 11*, 1203−1214.

(10) Rudolph, U., and Möhler, H. (2014) GABA$_A$ receptor subtypes: Therapeutic potential in Down syndrome, affective disorders, schizophrenia, and autism. *Annu. Rev. Pharmacol. Toxicol. 54*, 483−507.

(11) Engin, E., Benham, R. S., and Rudolph, U. (2018) An Emerging Circuit Pharmacology of GABA$_A$ Receptors. *Trends Pharmacol. Sci. 39* (8), 710−732.

(12) Braat, S., and Kooy, R. F. (2015) The GABA$_A$ Receptor as a Therapeutic Target for Neurodevelopmental Disorders. *Neuron 86* (5), 1119−30.

(13) Maramai, S., Benchekroun, M., Ward, S. E., and Atack, J. R. (2020) Subtype Selective γ-Aminobutyric Acid Type A Receptor (GABAAR) Modulators Acting at the Benzodiazepine Binding Site: An Update. *J. Med. Chem. 63* (7), 3425−3446.

(14) Hoestgaard-Jensen, K., Dalby, N. O., Krall, J., Hammer, H., Krogsgaard-Larsen, P., Frølund, B., and Jensen, A. A. (2014) Probing α4βδ GABA$_A$ receptor heterogeneity: differential regional effects of a functionally selective α4β1δ/α4β3δ receptor agonist on tonic and phasic inhibition in rat brain. *J. Neurosci. 34*, 16256−16272.

(15) Ramerstorfer, J., Furtmuller, R., Sarto-Jackson, I., Varagic, Z., Sieghart, W., and Ernst, M. (2011) The GABA$_A$ receptor α+β- interface: a novel target for subtype selective drugs. *J. Neurosci. 31*, 870−7.

(16) Martinez Botella, G., Salituro, F. G., Harrison, B. L., Beresis, R. T., Bai, Z., Blanco, M. J., Belfort, G. M., Dai, J., Loya, C. M., Ackley, M. A., Althaus, A. L., Grossman, S. J., Hoffmann, E., Doherty, J. J., and Robichaud, A. J. (2017) Neuroactive Steroids. 2. 3alpha-Hydroxy-3beta-methyl-21-(4-cyano-1H-pyrazol-1′-yl)-19-nor-5beta-pregnan-20 -one (SAGE-217): A Clinical Next Generation Neuroactive Steroid Positive Allosteric Modulator of the (gamma-Aminobutyric Acid)A Receptor. *J. Med. Chem. 60* (18), 7810−7819.

(17) Sieghart, W. (2015) Allosteric modulation of GABA$_A$ receptors via multiple drug-binding sites. *Adv. Pharmacol. 72*, 53−96.

(18) Olsen, R. W. (2015) Allosteric ligands and their binding sites define γ-aminobutyric acid (GABA) type A receptor subtypes. *Adv. Pharmacol. 73*, 167−202.

(19) Li, G. D., Chiara, D. C., Sawyer, G. W., Husain, S. S., Olsen, R. W., and Cohen, J. B. (2006) Identification of a GABA$_A$ receptor anesthetic binding site at subunit interfaces by photolabeling with an etomidate analog. *J. Neurosci. 26*, 11599−605.

(20) Belelli, D., Lambert, J. J., Peters, J. A., Wafford, K., and Whiting, P. J. (1997) The interaction of the general anesthetic etomidate with the γ-aminobutyric acid type A receptor is influenced by a single amino acid. *Proc. Natl. Acad. Sci. U. S. A. 94*, 11031−6.

(21) Wingrove, P. B., Wafford, K. A., Bain, C., and Whiting, P. J. (1994) The modulatory action of loreclezole at the γ-aminobutyric acid type A receptor is determined by a single amino acid in the β2 and β3 subunit. *Proc. Natl. Acad. Sci. U. S. A. 91*, 4569−73.

(22) Wafford, K. A., Bain, C. J., Quirk, K., McKernan, R. M., Wingrove, P. B., Whiting, P. J., and Kemp, J. A. (1994) A novel allosteric modulatory site on the GABA$_A$ receptor β subunit. *Neuron 12*, 775−82.

(23) Stewart, D., Desai, R., Cheng, Q., Liu, A., and Forman, S. A. (2008) Tryptophan mutations at azi-etomidate photo-incorporation sites on α1 or β2 subunits enhance GABA$_A$ receptor gating and reduce etomidate modulation. *Mol. Pharmacol. 74*, 1687−95.

(24) Stewart, D. S., Hotta, M., Li, G. D., Desai, R., Chiara, D. C., Olsen, R. W., and Forman, S. A. (2013) Cysteine substitutions define etomidate binding and gating linkages in the α-M1 domain of γ-aminobutyric acid type A (GABA$_A$) receptors. *J. Biol. Chem. 288*, 30373−86.

(25) Olander, E. R., Madjroh, N., Bunch, L., Soderhielm, P. C., and Jensen, A. A. (2018) Delineation of the functional properties and the mechanism of action of AA29504, an allosteric agonist and positive allosteric modulator of GABAA receptors. *Biochem. Pharmacol. 150*, 305−319.

(26) Krasowski, M. D., Nishikawa, K., Nikolaeva, N., Lin, A., and Harrison, N. L. (2001) Methionine 286 in transmembrane domain 3 of the GABA$_A$ receptor β subunit controls a binding cavity for propofol and other alkylphenol general anesthetics. *Neuropharmacology 41*, 952−64.

(27) Halliwell, R. F., Thomas, P., Patten, D., James, C. H., Martinez-Torres, A., Miledi, R., and Smart, T. G. (1999) Subunit-selective modulation of GABA$_A$ receptors by the non-steroidal anti-inflammatory agent, mefenamic acid. *Eur. J. Neurosci. 11*, 2897−905.

(28) Khom, S., Baburin, I., Timin, E., Hohaus, A., Trauner, G., Kopp, B., and Hering, S. (2007) Valerenic acid potentiates and inhibits GABA$_A$ receptors: molecular mechanism and subunit specificity. *Neuropharmacology 53*, 178−87.

(29) Luger, D., Poli, G., Wieder, M., Stadler, M., Ke, S., Ernst, M., Hohaus, A., Linder, T., Seidel, T., Langer, T., Khom, S., and Hering, S. (2015) Identification of the putative binding pocket of valerenic acid on GABA$_A$ receptors using docking studies and site-directed mutagenesis. *Br. J. Pharmacol. 172* (22), 5403−13.

(30) Chua, H. C., Christensen, E. T., Hoestgaard-Jensen, K., Hartiadi, L. Y., Ramzan, I., Jensen, A. A., Absalom, N. L., and Chebib, M. (2016) Kavain, the major constituent of the anxiolytic kava extract,

https://dx.doi.org/10.1021/acschemneuro.0c00600
ACS Chem. Neurosci. XXXX, XXX, XXX−XXX

potentiates $GABA_A$ Receptors: Functional characteristics and molecular mechanism. *PLoS One 11* (6), No. e0157700.
(31) Chiara, D. C., Jayakar, S. S., Zhou, X., Zhang, X., Savechenkov, P. Y., Bruzik, K. S., Miller, K. W., and Cohen, J. B. (2013) Specificity of intersubunit general anesthetic-binding sites in the transmembrane domain of the human $\alpha1\beta3\gamma2$ γ-aminobutyric acid type A ($GABA_A$) receptor. *J. Biol. Chem. 288*, 19343−57.
(32) Hilpert, K., Elliott, M. R., Volkmer-Engert, R., Henklein, P., Donini, O., Zhou, Q., Winkler, D. F., and Hancock, R. E. (2006) Sequence requirements and an optimization strategy for short antimicrobial peptides. *Chem. Biol. 13* (10), 1101−7.
(33) Hammer, H., Bader, B. M., Ehnert, C., Bundgaard, C., Bunch, L., Hoestgaard-Jensen, K., Schroeder, O. H., Bastlund, J. F., Gramowski-Voß, A., and Jensen, A. A. (2015) A multifaceted $GABA_A$ receptor modulator: Functional properties and molecular mechanism of action of the sedative-hypnotic and recreational drug methaqualone (Quaalude). *Mol. Pharmacol. 88*, 401−420.
(34) Madjroh, N., Olander, E. R., Bundgaard, C., Soderhielm, P. C., and Jensen, A. A. (2018) Functional properties and mechanism of action of PPTQ, an allosteric agonist and low nanomolar positive allosteric modulator at GABAA receptors. *Biochem. Pharmacol. 147*, 153−169.
(35) Bozdag, M., Alafeefy, A. M., Vullo, D., Carta, F., Dedeoglu, N., Al-Tamimi, A.-M. S., Al-Jaber, N. A., Scozzafava, A., and Supuran, C. T. (2015) Benzenesulfonamides incorporating bulky aromatic/heterocyclic tails with potent carbonic anhydrase inhibitory activity. *Bioorg. Med. Chem. 23* (24), 7751−7764.
(36) Dandia, A., Singh, R., and Sarawgi, P. (2005) Reinvestigation of the synthesis of 2-benzyl-3-aryl-quinazolin-4-[3 H]-ones. An improved multi-component procedure using microwaves. *Org. Prep. Proced. Int. 37* (4), 397−402.
(37) Saravanan, G., Alagarsamy, V., and Kumar, P. D. (2015) Synthesis and pharmacological investigations of novel 2-phenyl-quinazolin-4 (3H)-one derivatives. *Med. Chem. Res. 24* (1), 408−422.
(38) Wu, L., and Hartwig, J. F. (2005) Mild palladium-catalyzed selective monoarylation of nitriles. *J. Am. Chem. Soc. 127* (45), 15824−15832.
(39) Zhu, S., Noviello, C. M., Teng, J., Walsh, R. M., Kim, J. J., and Hibbs, R. E. (2018) Structure of a human synaptic GABA A receptor. *Nature 559* (7712), 67−72.

https://dx.doi.org/10.1021/acschemneuro.0c00600
ACS Chem. Neurosci. XXXX, XXX, XXX−XXX